Miguel Fernando Andrade Pinheiro

Licenciado em Engenharia de Micro e Nanotecnologias

Printable RF Antennas for Power Harvesting in Paper Electronics: Optimisation of Printable Materials and Substrates

Dissertação para obtenção do Grau de Mestre em

Engenharia de Micro e Nanotecnologias

Orientador: Dr. Luís Pereira, Professor Associado, Faculdade de Ciências e Tecnologias da Universidade Nova de Lisboa

Co-orientador: Dr. João Pedro Oliveira, Professor Auxiliar, Faculdade de Ciências e Tecnologias da Universidade Nova de Lisboa

FACULDADE DE CIÊNCIAS E TECNOLOGIA
UNIVERSIDADE NOVA DE LISBOA

Setembro de 2018

Printable RF Antennas for Power Harvesting in Paper Electronics: Optimisation of Printable Materials and Substrates

Faculdade de Ciências e Tecnologia

Universidade Nova de Lisboa

Acknowledgements

It is with an immense pleasure and satisfaction that I end this journey. This master thesis represents the end of a very long process. Many hours of study, memories and moments that will always remain.

Firstly, I would like to thank everyone that took part in this process, that helped me during this master thesis and during all this 5-year battle.

To Prof. Dr. Rodrigo Martins and Prof. Dr. Elvira Fortunato for the creation and divulgation of this new but highly reputable Engineering course. A special thank you also, for the opportunity of making my Master Thesis in those highly regarded facilities that are CENIMAT|i3N and CEMOP, where the investigation conditions are exceptional.

To my Advisor, Prof. Dr. Luís Pereira, a special thank you for all the support and for the opportunity to join this project and your team. Thank you for your help, advising and knowledge transmission.

To my Co-advisor Prof. Dr. João Paulo Oliveira and UNINOVA team for the help during this period and for the feedback given about the produced devices.

To all the group at paper laboratory: Paul, Diana, Inês, Raquel, Tiago, Marco and Joana. For all the hours we spent together, all the moments of fun, all the devices fabricated and the good state of mind you passed me.

To all the team at CENIMAT|i3N that helped during this period whenever I needed: Ana Pimentel, Rita Branquinho, Alexandra Gonçalves, Sónia Pereira, Joana Pinto, Daniela Salgueiro and Marta Ferreira.

To my two supervisors, Cristina Gaspar and João Ribas. For all the hours discussing the next step, for all the advising you gave and for all the dedication towards me. Without you, this work would never be possible. I owe you a lot.

To all the friends I made throughout this course. For all the hours we spent together, all the moments of fun, talks and the stuff we've been through together, I will always remember those moments and you: André, Recife, Marta, Nuno Ferreira, Casa Branca, Inês, Bernardo, Neto, Matos, Glória, Rui, Nia, Tomás, Mariana and the "runaways" João Pina and Miguel Ramos.

To Sergio, Tiago and Ana for the friendship of many years. You've been here since almost day one. To my house colleagues and the "appendixes" over these 5 years. With you guys this journey became a lot funnier. All the moments of joy will be always remembered, as well as, all the episodes of craziness: Sobral, João, Quiry, Pedro and specially, João Calão.

To my girlfriend Filipa, thank you for all the advises and motivation. These five years went flying and I'm glad you were by my side in this process. You made me a lot happier and helped me a lot during this period. Thank you, a lot.

To my sister Ana and my brother-in-law Jorge, for all the support you gave me throughout this journey and the good mood you passed me. To Artur, my nephew, that made the end of this journey much happier.

Finally, I would like to give a special thanks to my parents, without whom this journey would be impossible. Without them I would not be the person I am today and without their effort this experience would never have happened.

Thank you all.

Abstract

This work documents the optimisation and fabrication of Radio Frequency Identification (RFID) antennas on paper substrates to be adapted and used at 13.56 MHz. The optimisation of the antenna layout was made by inkjet printing and after that compared with two other printing techniques: flexography and screen printing. Commercial silver (Ag) nanoparticles (NPs) based inks were used to obtain conductive paths. The inkjet ink was characterised by Thermogravimetric Analysis and Differential Scanning Calorimetry (TGA-DSC) and Viscometer to know the effect of temperature on the ink components. Absorbance measurements were also done from 200 to 800 nm to know at which wavelength more energy is absorbed by the ink, which had a maximum peak at 320 nm. Three different types of paper were studied (Office, INCM Coated and INCM Uncoated) and morphologically characterised by TGA-DSC, Scanning Electron Microscopy with Energy Dispersive Spectroscopy for surface element detection and profilometry for surface roughness study. From the studied papers, INCM Coated paper presented an average roughness of 1015 nm and hydrophilic behaviour with a 68.8º contact angle. It also showed better resistance to the temperature when compared with Office and INCM Uncoated paper. The layout suffered different modifications over time to ease the inkjet fabrication and reduce the pad-to-pad resistance. The final design was used in the three printing techniques. Inkjet printing showed higher resolution and printing quality, although the printing process and the sintering time were slower. For inkjet, INCM Coated was the paper that better exhibited the least resistive conductive paths, reaching 106 Ω. Office and INCM Uncoated lowest resistance values reached 140 Ω for that technique. Interesting results were obtained by screen printing, in which all the selected substrates presented low values between 17 Ω and 35 Ω. With this, the objective was achieved, since RFID antennas were successfully produced, and a proof of concept was done.

Keywords: RFID, paper electronics, printed electronics, inkjet printing, screen printing, flexographic printing.

Resumo

Este trabalho documenta a otimização e fabricação de antenas de Identificação de Radiofrequência (RFID) em substratos de papel para serem adaptadas e utilizadas a 13,56 MHz. A otimização do formato da antena foi feita por impressão de jato de tinta e posteriormente comparada com duas outras técnicas: flexografia e serigrafia. Foram utilizadas tintas comercias à base de nanopartículas (NP) de prata (Ag) para obter pistas condutoras. A tinta utilizada em impressão de jato de tinta foi caracterizada por análise termogravimétrica e calorimetria de varrimento diferencial (TGA-DSC).Também foi usado o viscosímetro de maneira a saber-se qual o efeito da temperatura nos componentes da tinta e por absorvância dos 200 aos 800 nm de maneira a saber-se qual o comprimento de onda em que a tinta absorve mais energia, que teve um pico máximo para o comprimento de onda de 320 nm. Foram estudados três substratos tipos de papel diferentes (Office, INCM Uncoated e INCM Coated) e caracterizados por TGA-DSC, microscopia eletrónica de varrimento com espetroscopia de energia dispersiva para deteção elementar à superfície e perfilometria para estudo de rugosidade. Dos papéis estudados, INCM Coated apresentou uma rugosidade de 1015nm e comportamento hidrofílico com um ângulo de contato de 68.8^{o}. Mostrou também melhor resistência a temperatura quando comparado com Office e INCM Uncoated. O formato da antena sofreu diversas modificações ao longo do tempo de maneira a facilitar a fabricação por impressora de jato de tinta e a reduzir a resistência entre contactos. O formato final foi impresso pelos três processos. A impressão por jato de tinta demostrou uma maior resolução e qualidade de impressão, no entanto, o processo foi mais lento bem como o tempo de sinterização. Para impressão de jato de tinta, INCM Coated foi o papel que obteve pistas com menor resistência, chegando aos 106 Ω. Os valores mais baixos obtidos para Office e INCM Uncoated foram por volta dos 140 Ω para a mesma técnica. Resultados interessantes foram obtidos por serigrafia, na qual, todos os substratos usados apresentaram baixos valores de resistência entre 17 Ω e 35 Ω. Com isto, o objetivo foi atingido visto que antenas de radiofrequência foram produzidas com sucesso e uma prova de conceito foi efetuada.

Palavras-chave: RFID, eletrónica em papel, eletrónica impressa, impressão por jato de tinta, serigrafia, flexografia.

Table of Contents

List of Figures

List of Tables

List of Abbreviations

CEMOP	Centro de Excelência de Microeletrónica, Optoeletrónica e Processos
CENIMAT|i3N	Centro de Investigação de Materiais | Instituto de Nanoestruturas, Nanomodelação e Nanofabricação
DPI	Dots per Inch
DSC	Differential Scanning Calorimetry
EDS	Energy Dispersive Spectroscopy
IC	Integrated Circuit
INCM	Imprensa Nacional – Casa da Moeda
IR	Infrared
NFC	Near Field Communication
NP	Nanoparticle
PC	Polycarbonate
PE	Printing Electronics
PEN	Polyethilene Naphtalate
PET	Polyethilene Terephtalate
PVD	Physical Vapor Deposition
PoP	Pen-on-Paper
PVP	Plyvinil Pyrolidone
R2R	Roll-to-roll
RFID	Radio Frequency Identification
RT	Room Temperature
S2S	Sheet-to-sheet
SEM	Scanning Electron Microscopy
TGA	Thermogravimetric Analysis
UV	Ultraviolet
Vis	Visible

Motivation

Technology is always evolving to accommodate the demand of a simpler and better quality of life. For example, nanotechnology has advanced by leaps and bounds over the last 15 years and it's exactly in this area that the focus of this work is centred.

Nanotechnology is a relatively new concept and its "definition" was first proposed by Richard Feynman, at the annual American Physical Society in December 29, 1959, in his lecture, "T*here's Plenty of Room at the Bottom.*[1] Nowadays, the term nanotechnology consists in the manipulation of materials and devices at a molecular level, reaching the nanometre scale (10^{-9} part of metre). After its concept's creation many doors, full of new devices and possibilities, have opened revealing solutions to many problems. Examples of that are the constant evolution of displays, paper and printing electronics, transparent and flexible electronics, biosensors, microfluidics among many other advances in several areas.

With the constant evolution of technology, new concepts are constantly showing up. One example is Internet of Things (IoT), the interconnection between daily life devices through internet, proposed by Ashton in 1999.[2] This represents a new era of evolution and is already being used with synchronization between smartphones, televisions, smartwatches, or even, washing machines.[3] In the Figure 1 below, the expected evolution for IoT is represented.

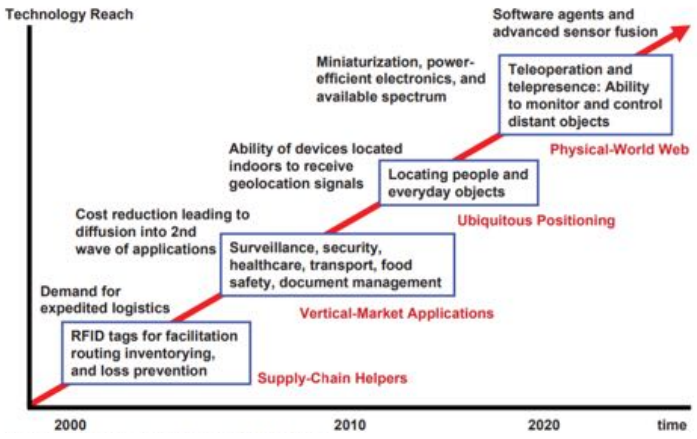

Figure 1 - Internet of Things technology roadmap.[4]

Radio Frequency Identification (RFID) antennas play an important role in IoT. They are capable of long-range identification, tracking, among many other applications. This technology can be the beginning of a new era with surrounding communication systems, intelligent devices and tracking systems.[5]–[8]

Until now, plastic substrates have been used vastly when it comes to flexible electronics, however, its use is ecologically questionable as it is non-biodegradable. Paper is a low-cost, environmentally friendly, recyclable and biodegradable substrate and with these properties a huge advance in technology can happen when mixed with the RFID systems.

Objectives

The main objective of this dissertation was to optimize the printing parameters and produce RFID antennas by inkjet printing. The goal was to achieve antennas with the closest to 50 Ω pad to pad resistance value, to be adapted and used at 13.56 MHz.

To give a better understanding of this work the main objective was divided in four secondary objectives:

- Study and characterisation of the substrates and inks used;
- Optimisation of the layout of the RFID antenna for inkjet printing;
- Comparison between the optimized layout with flexographic and screen printing techniques;
- Frequency analysis of the printed RFID antennas produced.

1 Introduction

To have a better comprehension of this work, a theoretical introduction will be presented in this section. The most important topics covered are related to paper, printing techniques and the Radio Frequency Identification (RFID) tags.

1.1 From Cellulose to Paper Electronics

Cellulose is the main structural component of paper. Cellulose $(C_6H_{10}O_5)_n$, is an organic compound and it is an unbranched polysaccharide chain of D-glucose units linked by β 1-4-glycosidic connections. It is the most abundant biopolymer on Earth and can be extracted from a wide range of sources such as cell walls (in wood), tunicate (a sea organism) or bacteria (which produces cellulose biofilms).[9] Cellulose has its applications on a wide range of areas, since paper fabrication to chemical industry, textile industry or even in pharmaceutics for drug production.[10],[11]

After wood chopping, to manufacture paper, the formation of pulp is required. That process can be performed in two ways: mechanically or chemically. In the mechanical process, wood-containing pulp is formed, since lignin is present. This process consists in grinding the wood until small fibres are obtained. It can be assisted by steam, (thermomechanical process) reducing the energy spent during the process.[12] The chemical process forms a wood-free pulp (without lignin) only containing cellulose fibres and can be done in various ways. The most common used is Kraft process where an aqueous solution of sodium hydroxide and sodium sulphide (known as white liquor) is used. This solution dissolves the lignin, which can be extracted after washing. [13]

After the pulp formation, the pulp is bleached to become whiter and eliminate the remaining lignin. This is the main cause for paper ageing (the degradation of paper, normally noticed by the paper turning yellow).[14] Some additives can be mixed with the paper to improve some characteristics like pigments and dyes to improve appearance and brightness, resins to improve the strength, between others. The resultant mixture goes to a paper machine, where the paper will be produced. In this machine, the mixture is dried and pressed with cylinders. The result emerges as paper webs (very large sheets). Paper manufacturing in these machines can achieve velocities rounding 100 km/h.[15]

Cellulose based materials, as substrate, present several advantages: low-cost, environmentally friendly, biodegradable and good mechanical proprieties such as flexibility. Although it has some drawbacks, associated with its roughness and porous surface, resulting in lower device performance when compared with non-porous substrates. [16]

1.2 Printing Techniques

In the last few decades, printing processes research has been evolving continuously due to the constant demands of new materials, methods and techniques to produce electronics. Those processes are divided in two groups: contact printing and non-contact printing. Contact printing consists in transferring the desired pattern through a mould which directly contacts the substrate. Contrarily, in the non-contact processes the ink passes through openings which have the desired to be transferred, without being in contact with the substrate. [17] The printing techniques and their respective classification are shown in Figure 2.

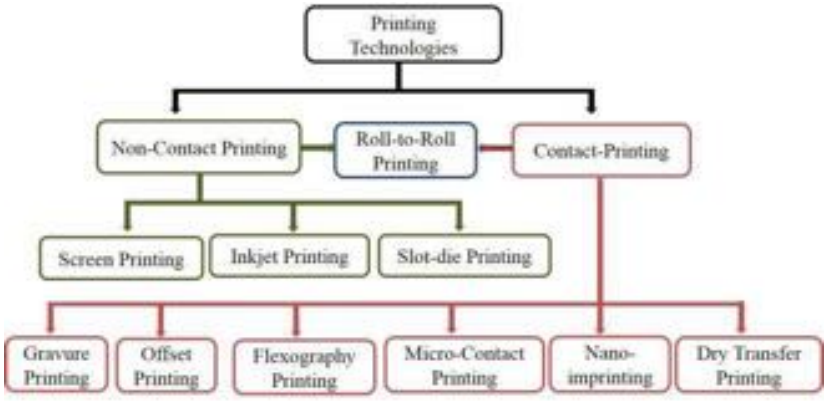

Figure 2 – Contact and non-contact printing techniques division.[18]

The objective of the printing techniques is the scalability to the industry for a roll-to-roll (R2R) process.[15],[19],[20] All the presented techniques have different characteristics, such as the obtained resolution, printing speed, ink characteristics, applicable area, among others. Some of these parameters are shown in Table 1.

Table 1 – Printing Techniques comparison in a wide range of parameters. Adapted from [18].

	Gravure	**Offset**	**Flexography**	**Micro contact & Nanoimprint**	**Transfer Printing**	**Screen**	**Inkjet**	**Slot-die**
Resolution (μm)	50-200	20-50	30-80	1-20	4-50	30-100	15-100	200
Thickness (μm)	0.02-12	0.6-2	0.17-8	0.006-0.6	0.23-2.5	0.6-100	0.02-5	0.6-5
Printing speed (m/min)	8-100	0.6-15	5-180	0.006-0.6	N/D	0.6-100	0.02-5	0.6-5
Solution viscosity (cPs)	10-1100	500-2000	10-500	~ 100	N/D	500-5000	1-100	2-5000
Superficial Tension(mN/m)	41-44	-	13.9-23	22-80	N/D	38-47	15-25	65-70
Controlled Environment	Yes	Yes	Yes	No	Yes	No	No	No
Printing area	Large	Large	Large	Medium	Medium	Medium	Large	Large
Material Wastage	Yes	Yes	Yes	Yes	No	Yes	No	Yes

1.2.1 **Inkjet Printing**

Inkjet is one of the most efficient and versatile printing techniques used nowadays, due to the high resolution presented in a wide range of substrates such as glass, polymer and paper.[15] This technique can have two different mechanisms: Continuous Inkjet (CIJ) and Drop-On-Demand (DOD) Inkjet. CIJ consists in applying a constant external electric field, while it produces a continuous stream of liquid drops; and unwanted drops can be removed by a gutter.[21],[22],[23]

DOD mechanism consists in a controlled drop method, in which the droplet only forms when desired. DOD can be split in thermal inkjet printing and piezoelectric inkjet printing. Thermal inkjet is a mechanism in which a thin film that is in contact with the ink is heated to a temperature above the ink boiling point, causing the ink to evaporate and to form a bubble that will force the droplet to shape and be released. In piezoelectric inkjet, a piezoelectric membrane is present in the nozzle and the droplet only takes shape when the membrane is deformed due to an applied voltage. Figure 3 shows a representation of thermal (on the left) and piezoelectric (on the right) DOD inkjet printing.[24],[25]

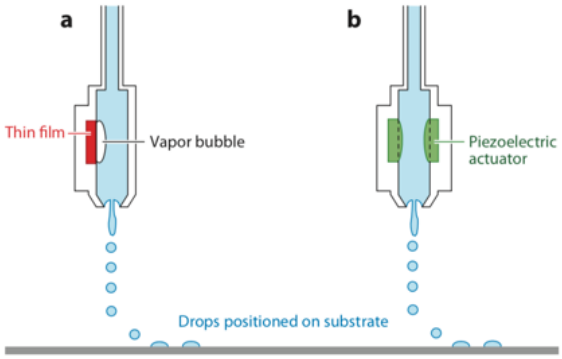

Figure 3 – Inkjet printing DOD mechanism: a) thermal b)piezoelectric. [21]

Ink viscosity depends on the printer's mechanism. A conventional office inkjet printer uses inks with a range of viscosities between 1-2 cPs. For research, those piezoelectric inkjet printers' viscosity values change and can reach 10-20 cPs, as seen in Table 1. [18],[25]

Inside inkjet printing the principal parameters to control are resolution, number of layers, substrate temperature and printing direction. The resolution (DPI) controls the number of dots per inch of ink droplets. The higher this value, higher the amount of dropped ink and consequently the printing time required. The number of layers consists in the number of times the printer sweeps the desired pattern inserted in the software. This value needs to be the smallest possible to reduce the printing time. Finally, the substrate temperature is the temperature set in the sample support plate, which causes a small evaporation of the solvent and consequently less scattering and absorption. For this reason, this parameter is highly related with the ink absorption by the fibres and the scattering of the ink when reaching the substrate. [15], [20], [24], [26], [27]

1.2.2 Flexographic Printing

Flexographic printing consists in transferring the ink to a substrate in a R2R process. This technique uses three rolls and a doctor blade. The first roll is the anilox, with the particularity of having thousands of cells with a fixed volume.[28] These cells can have different formats such as hexagonal, square, quadrangular, among others and are filled with ink by drop casting, with the excess being removed by the doctor blade. While rotating, the ink is transferred to a second roll, which has a mask with the desired pattern. As shown in Figure 4 the ink only covers the upper parts of the pattern and is then deposited on the substrate. As the name implies, flexographic needs a flexible substrate, which is more a constrain than a disadvantage, as there are many substrates that can be used like paper, cork or polymeric.[29] The viscosity values are set in a wide range of values, 10-500 cPs, due to its versatility and many anilox volume rolls available, as shown on Table 1. [18]

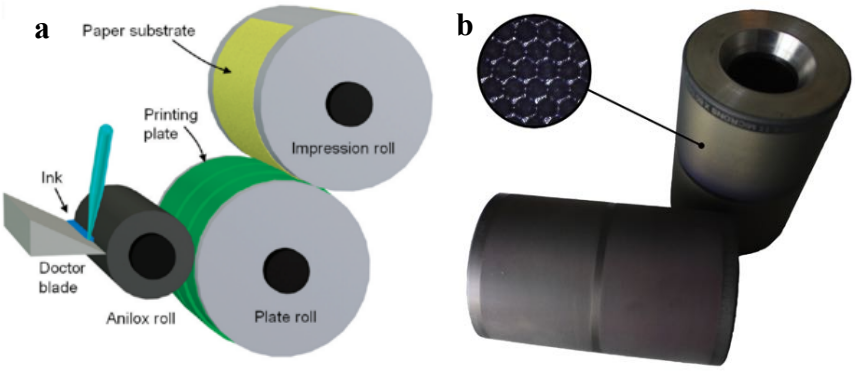

Figure 4 – a) Flexographic printing schematic, in black the anilox roll, in green the mask and the substrate in yellow. [29] b) Two anilox rolls with cell zoomed.[28]

There are two more parameters to take in consideration in flexographic printing, these are associated with the pressure between rolls, and can be from 1 to 200, with 200 the one that exercise more pressure.

1.2.3 Screen Printing

In screen printing, the ink, commonly referred to as paste, is pressed with a squeegee through a net called “mesh” onto the substrate. The image to be replicated is generally made photochemically using photolithography processes, directly in the mesh. Due to the simplicity of the process, a wide variety of substrates (from flexible to rigid ones) and inks can be used. High viscosity inks allow a thicker layer when compared with other printing techniques. [30] Figure 5 shows the schematic for the screen printing process.

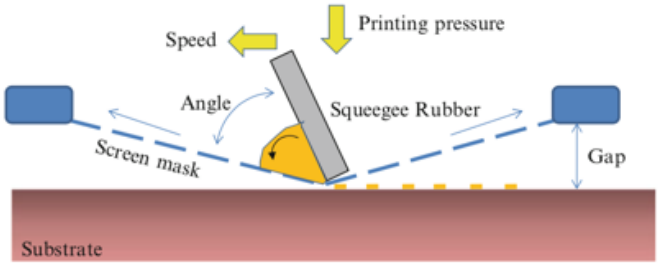

Figure 5 – Screen printing technique schematic. [20]

Screen printing can be divided in two sub-categories: manual and automatic screen printing. In manual screen printing, ink is pressed by the user and the result relies heavily on the physical abilities of the operator therefore there are parameters that may differ. Those are the alignment, the pressure, speed and angle applied on the squeegee. These parameters can also change throughout the printing processes. In automatic screen printing the variables concerning to the operator are reduced. Since this process is automatic it consists in a mechanic arm that does the process instead of the user and camera assisted alignment. Therefore, the force, printing velocity and other parameters concerning to the squeegee are programmed and those are fixed values set by the operator. It is expected to have better reproducibility than manual screen printing and to be faster due to the automaticity of the all process and alignment easiness.[31],[32]

1.3 Sintering

Printed Electronics (PE) demands conductive paths. To achieve that, the inks need to be sintered to remove the solvent and the NPs capping.[33] This capping is made of polymer-based agents, usually PVP. It is used to avoid the aggregation of the NPs in storage.[34] This procedure is called sintering. For each ink there is a suitable sintering process suggested by the ink supplier. Nowadays, the most common sintering processes used with Ag NPs inks are photonic-sintering (Infrared sintering), Ultraviolet (UV) sintering, hot-plate sintering and oven sintering.[35],[36],[37],[38],[39]

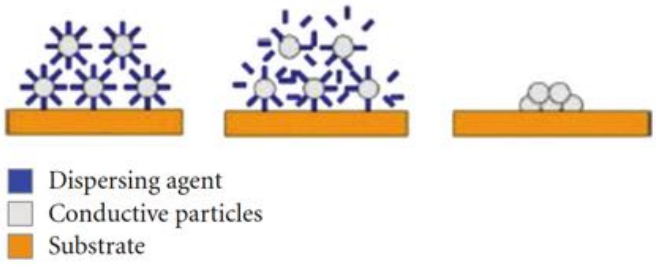

Figure 6 - Sintering process schematic.[40]

1.4 Printing Electronics Applications

Currently PE presents high capacity in replacing current mass production electronic modules. It has a wide range of applications on flexible substrates and they are present on: packaging, diagnostics, RFID antennas [41],[42], transistors [43],[44] , sensors [16],[45], just to highlight a few. As shown in Figure 7 there are many applications for these techniques.

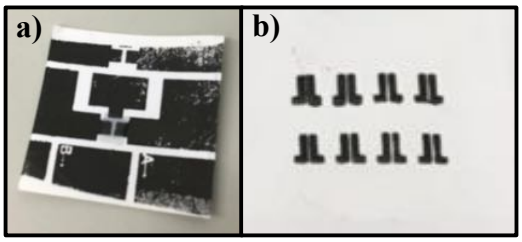

Figure 7 - Paper Transistor (a) and paper UV sensor (b) made in CENIMAT / i3N.

1.4.1 RFID – Radio Frequency Identification

The Radio Frequency Identification (RFID) concept remotes to the 19th century with the discoveries of Faraday and Maxwell (inductance and magnetism, respectively). Radio Detection and Raging, commonly known as RADAR was invented by Henry Stockman [46] and it is widely known. This turned out to be a good asset at military levels and later, during World War 2, was called by the British Royal Air Force as IFF, Identify Friend or Foe, since the pilots could identify the other planes with RF signals.[46]

The RFID system is composed by 3 main elements: the RFID tag (antenna), a reader and a database. The reader is the source of the RF wave, usually producing the signal that will be received in the antenna and receiving it back to store it in the database. [5]

There are three types of antennas: passive, semi passive and active. The main factor that decides which one it is concerns to its power source, as shown on Table 2. The active antennas have a battery that powers all its functions, the semi passive also has a battery but only to turn on the IC and last, the passive antennas do not have any IC neither a battery. Although making the tag cheaper, it has less operating range. [46],[47]

Table 2 - Comparison between the 3 types of RFID antennas: passive, semi-passive and active.[46]

	Passive	**Semi-passive**	**Active**
Source	Harvesting RF	Battery	Battery
Communication	Answer only	Answer only	Starter and answer
Maximum Range	10 m	> 100 m	> 100m
Relative Cost	-	+	+ +
Applications (example)	Proximity cards	Tracking	Tracking

In this work, passive RFID antennas were produced, so batteries are not necessary. The minimal distance for those RFID antennas to be functional depends on its frequency, as well as the maximum distance those antennas can be from the signal source, as shown in Table 3. The operation frequencies used in RFID are divided in five major categories being those: low-frequency, high-frequency, ultra-high-frequency, microwave and ultrawide band.

Table 3 – Operation frequencies and respective read distance. [48]

	Frequency Range	**Passive Read Distance**
Low Frequency (LF)	120-140 kHz	10-20 cm
High Frequency (HF)	13.56 MHz	10-20 cm
Ultra-high Frequency (UHF)	~900 MHz	3 m
Microwave (MW)	2.45-5.8 GHz	3 m
Ultra-wide Band (UWB)	3.1-10.6 GHz	10 m

1.4.2 **RFID Manufacturing**

The most common way to fabricate RFID antennas is PVD (Physical Vapor Deposition) and thermal evaporation techniques. [49] These processes are very efficient, but the overall cost and energy spent are some of the drawbacks. So, the constant need to optimize production, minimize costs and use sustainable resources, demands the use of fast, low-cost and mass-production techniques.[50],[51],[52] PE represents itself a great candidate to substitute conventional clean room techniques, with its great advantage. One PE technique that stands out is inkjet printing, which offers remarkable improvements in this area, with high resolution, extremely controlled process and the uniqueness of testing various designs without the need of producing masks, as it is required in screen printing and flexographic printing.[15], [18], [29], [53]

RFID antennas are present in many objects in our daily life and can be observed in shopping control on clothes, payment methods, library systems, real time tracking, inventory control, documents control, fast payment methods and public transports cards are just some examples. The trend is the RFID to be more embedded in daily life products. Figure 8 shows two examples of the use of RFID in every day's consumer items, a public transports card and a Via Verde receiver, used for toll pay in Portuguese highways.[54]

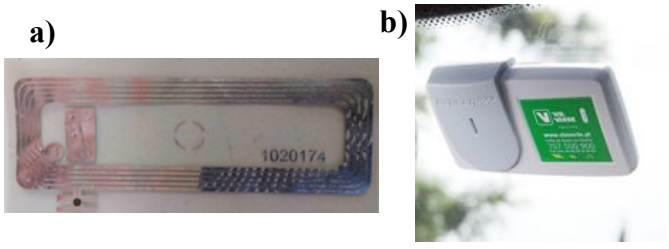

Figure 8 – RFID antenna present in public transport card (a); Via Verde receiver which main component is an RFID antenna. [55]

2 Materials and Methods

This section presents all the steps taken to produce the RFID antennas on paper substrates, as well as its printing process parameters. The characterisation processes parameters will also be presented.

2.1 Substrates

Three different paper substrates were selected for comparison of their proprieties and feasibility as a possible substrate for PE. Those are Office paper, INAPA Tecno Super Speed 80 g/m^2 produced in Portugal by INAPA [56] and two papers provided by Imprensa Nacional-Casa da Moeda [57] : INCM uncoated paper, commercially named Arjo Wiggins 120 g/cm^2 and INCM coated paper, INAPA Imagine Silk 300 g/m^2.

2.2 RFID Antenna Printing Process

The complete RFID antenna consists of a 3-layer printing process and it's shown in Figure 9. In black is represented the first layer, which consists in a conductive track, is followed by an insulant layer, necessary to pull the inside pad to outside of the loop avoiding short circuit with the antenna coil (represented in blue) and to finalise, in orange, a conductive path which brings the inner pad to outside the coil.

Figure 9 - RFID antenna 3-layer layout. In black is represented the first layer (antenna coil), in blue the insulant bridge (second layer) and in orange the last layer that pulls the inner pad to outside of the coil.

2.2.1 Inkjet Printing

The printing was carried out by PixDro LP50 inkjet printer with the adaptation for the Dimatix 11610 printheads, which has 16 nozzles, that forms a 10pL droplet corresponding to approximately 30 µm diameter droplet. The range of viscosities supported by the printer are between 10 and 20 cPs, according to the manufacturer's specifications.[58]

The frequency used was fixed at 500 Hz and the printing velocity was fixed at 200 mm/s. Y direction was selected as printing direction and the process was bidirectional. Resolution values varied from 1000 and 2000 dpi and the substrate plate temperature was from room temperature (RT) up to 75 ºC depending on the substrate.

A silver (Ag) nanoparticles-based ink was used, Sicrys I50T-13, from PV Nanocell. The ink has a 50 w% of Ag NPs (average size between 70-115 nm) and expected viscosity 26 cPs at 25 ºC, according to the manufacturer. According to the manufacturer's specifications the ink sintering process is 200 ^{o}C for 30 minutes.

2.2.2 Flexographic Printing

FLEXIPROOF 100 from RK Printcoat Instruments with WB1078 Ag NPs ink from Applied Ink Solutions were used for printing the conductive layer. [59] The initial viscosity values were around 4000 cPs, so the ink was diluted in a 2:1 with ultrapure water. The sintering, according to the ink supplier, is 2 minutes at 145 ºC in hot plate. [60]

Printing velocity was 40 m/min. The pressure values were fixed at 150 between the anilox and the mask roll and 100 between the mask and the substrate. The sample substrate anilox and mask have the length and half the width of an A4 sheet, making it 105 mm x 297 mm.

2.2.3 Screen Printing

The mesh used was model 77 and the printing angle was approximately 45^{o}. The screen printing conductive ink used was CRSN2442 produced by SunChemicals and, as the other inks used, was also Ag NPs based. The viscosity of this ink comprehended between 2000 and 3000 cPs. The suitable sintering process is 120 ^{o}C for 2 minutes, according to the fabricant. [61] For the insulant bridge, also by SunChemicals, the CFSN6057 UV Coverlay was used. The optimal curing for this ink consists of 650mJ/cm^2 achieved by a two lamp 100 W/cm UV drier. According to the supplier, these two inks have a good behaviour when overprinted.[62]

2.3 Characterisation Techniques

Scanning Electron Microscopy (SEM) images were obtained with Tabletop microscope TM3030 Plus, with the Quantax 70 Energy Dispersive X-Ray Spectrophotometer (EDS). The SEM images and the EDS measurements were taken with an acceleration tension of 15 keV. The 3D scanning profilometry was performed using Ambios XP-plus 200 profiler in a 0.5 × 0.5 mm^2 area.

Thermal characterisation of substrates and inks was performed by thermogravimetric analyses (TGA). The paper samples were loaded in the thermal analyser TGA-DSC-STA 449 F3 Jupiter at atmospheric pressure and then heated from room temperature to 550 ºC, with a 5 ºC/min step.

Contact angle measurements were carried out using Dataphysics OCA-15plus, applying 1 µl of ultrapure water to the surface of the papers in study. The method used was sessile drop that consists in dropping a droplet on the substrate to evaluate its wettability.

Viscometer measurements were carried out using Brookfield CAP2000+ viscometer. The temperature sweep started at room temperature up to 50 ºC with a 0.2 ºC/second step.

Ink absorbance was measured using the UV-Vis-NIR spectrophotometer Shimadzu UV 3101pc from 230 to 850 nm wavelength.

DC electrical resistance of each antenna was measured pad-to-pad using the multimeter as an ohmmeter UNI-T UT33D Digital Multimeter.

The RFID antennas produced were characterized with Agilent 4294A Precision Impedance Analyzer to evaluate their behaviour in frequency from 1 to 60 MHz. The produced voltage of each antenna was measured with Arduino Uno using an RFID Reader RC522.

3 Results and Discussion

3.1 Paper Substrates Analysis

In the Figure 10 below is represented all three types of paper used. From left to right, office paper, INCM uncoated paper and INCM coated paper.

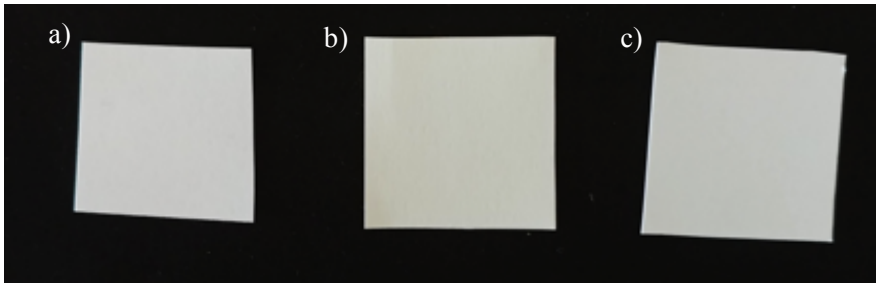

Figure 10 - Paper substrates selected: a) office paper; b) INCM uncoated paper; c) INCM coated paper.

3.1.1 Contact Angle

To have a better understanding of the behaviour of a droplet when it reaches each substrate, contact angle measurements were performed, using the sessile drop method and ultrapure water. Contact angle measurements are presented in Table 4 below.

Table 4 - Contact angle measurements for 5 droplets.

	Office Paper	**INCM Uncoated Paper**	**INCM Coated Paper**
Contact Angle (º)	100.1 ± 3.3	119.5 ± 5.8	68.8 ± 0.6

INCM Coated is the only paper that presents a contact angle smaller than 90º, which indicates that its surface may be smoother than the other two papers that are hydrophobic. INCM Uncoated paper having a contact angle of approximately 120º, can be considered a super-hydrophobic surface. This can indicate fibres and fillers presence in the substrate surface.

3.1.2 Paper Thickness

In Table 5 is represented the thickness values of all paper substrates. Each substrate was measured 10 times in different sheets and different spots. When compared, this can bring some differences in the final antenna, such as the weight, ink absorption, paper ageing and sintering difficulty.

Table 5 - Thickness values for each type of paper.

	Office Paper	**INCM Uncoated Paper**	**INCM Coated Paper**
Thickness (μm)	100.20 ± 2.70	149.00 ± 1.70	264.50 ± 3.84

3.1.3 Surface Analysis

3.1.3.1 SEM/EDS imaging

Paper surface represents a major property in PE, as directly influences if a device works properly. SEM images were taken to determine the wettability and surface morphology of the used substrates. These images as well as the EDS spectrum for the respective substrates are shown in Figure 11 to Figure 13. EDS scan results are shown in more detail in Annex A.

Office paper presents a matrix of fibres with different dimensions averaging 9.6 µm irregularly distributed. Shows also porosity and some amount of fillers. Concerning the EDS, the elements detected are carbon (C), oxygen (O) and calcium (Ca), this happens due to the calcium carbonate ($CaCO_3$), commonly used in the paper industry.

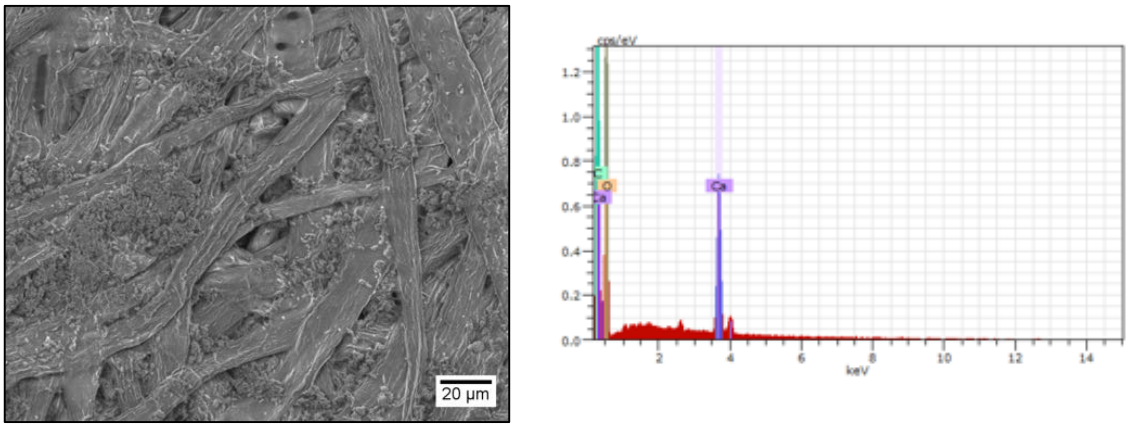

Figure 11 – SEM image of Office paper (a) and respective EDS spectrum (b).

INCM Uncoated paper shows less fibres than Office paper, with an average width of 15,7 µm but bigger amount of fillers. This paper seems also to be more compact due to the reduced holes between fibres. The EDS results do not show Ca presence, this can be the cause of its normal yellow colour and it is related to the fabrication process.

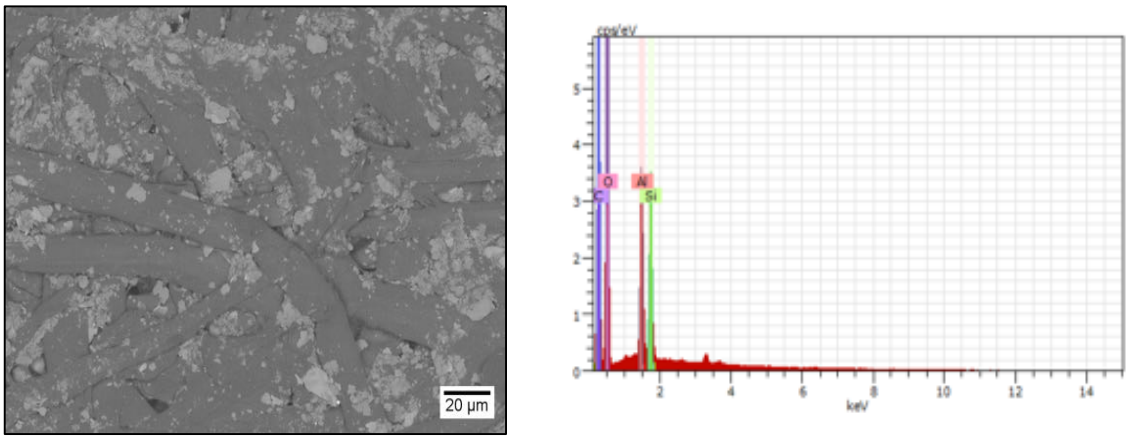

Figure 12 - SEM image of INCM Uncoated paper (a) and respective EDS spectrum (b).

In the Figure 13 below is represented the last paper substrate used. INCM Coated paper presents a smoother surface which can imply the existence of a coating, since there is no presence of fibres, only some holes and cracks with different diameters. A cross-section of this substrate is represented in Annex B.

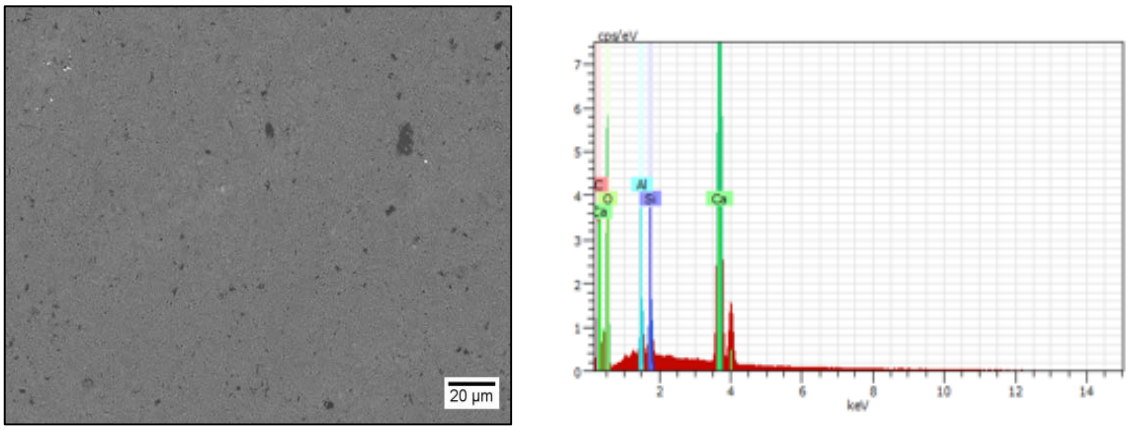

Figure 13 - INCM Coated paper SEM images (a) and respective EDS spectrum (b).

For PE applications INCM Coated paper is expected to have a better behaviour due to the coating preventing large absorption and scattering of the ink through the fibres. Although, this coating can represent less ink adhesion to the substrate.

In both INCM Coated and Uncoated papers there is a presence of aluminium (Al) and silicon (Si), this not only, may have to do with the mechanical fabrication process where the wood is grinded with artificial stones made of silicon carbide (SiC) or aluminium oxide (AlO) grits. [63] but also can be a sign of external contamination. In the two substrates that do not have any coating (Office paper and Uncoated Paper) it is expected from them to have more ink absorption and scattering.

3.1.3.2 Profilometry

Although SEM analysis can show the surface morphology of the substrates, the profilometry can give more information of roughness and quantify it. [64]

3D scans results performed in a 0.5 × 0.5 mm^2 area are represented in Figure 14. The profiler software measurements are presented in Table 6. Office paper proves to be the more irregular as expected after the SEM images as shown in Figure 14 a). The variations in depth have to do with the fibres at the paper surface. When compared with INCM Uncoated paper, in Figure 14 b), office paper presents less surface roughness but higher peak to valley height. The INCM Uncoated roughness being higher than the office paper is probably related to the filler's presence at the surface. The INCM Coated paper represented in Figure 14 c) presents very different values when compared with both office and INCM Uncoated paper. These values are substantially lower and

confirm what was expected with the SEM images: a very smooth surface. As said before, this fact can be due to a surface coating presence.

Table 6 - Peak to valley height (nm) and average roughness (nm) for each substrate used. Measurements obtained by Ambios XP-plus 200 Profiler software.

	Office Paper	Uncoated Paper	Coated Paper
Peak to valley height (nm)	51179	48219	11072
Roughness (nm)	3096	4355	1015

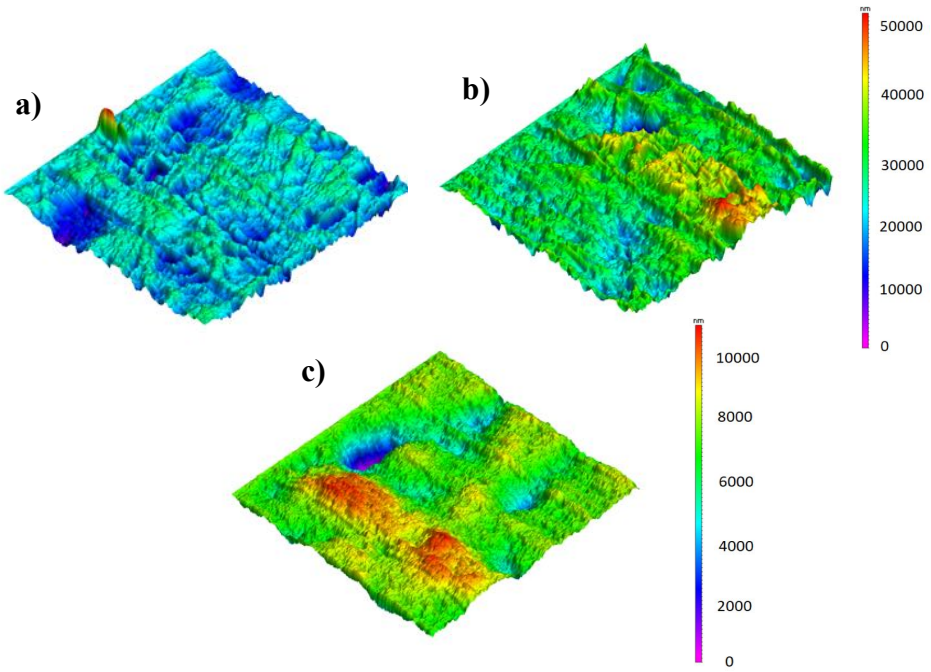

Figure 14 - Profilometry images of (a) office paper, (b) INCM Uncoated paper and (c) INCM Coated paper.

3.1.4 TGA-DSC Analysis

TGA-DSC analysis was performed to the three paper substrates and the results were plotted and shown in the Figure 15. This type of analysis is essential to know at which temperature the substrate loses more mass percentage and know its behaviour with increasing temperature. Since the ink will need a sintering process that effectively removes the capping from the NPs, to form a conductive path, the ink will be submitted to high temperatures and consequently the substrate. This will cause paper ageing which means paper degradation, a phenomenon usually associated with the change of colour in the paper to yellow. The thermal decomposition of cellulosic substrates consists on the degradation of its components: Hemicellulose decomposition, lignin pyrolysis, depolymerisation of cellulose, combustion and char oxidation.[65]

INCM Coated paper presents almost no weight lost in inert atmosphere. The DSC only shows two relevant peaks at 280 ºC and 350 ºC, corresponding to the beginning and finishing of a 10%

weight loss relative to the cellulose degradation. INCM Uncoated paper and Office paper have similar behaviours in both analyses. Although Office paper starts losing weight sooner, the % mass loss is approximately the same in both substrates, around 50%. The mass continues to decrease reaching 30% at 550ºC. DSC for these papers present one peak near 280 ºC. Although INCM Uncoated and Office have the same final percentage, since they have different initial masses, INCM Uncoated paper is still heavier than Office. These final masses are related to the mixture of additives during paper manufacturing.

Based on these results the sintering temperature for all three substrates should not exceed 250 ºC to not damage the paper substrate.

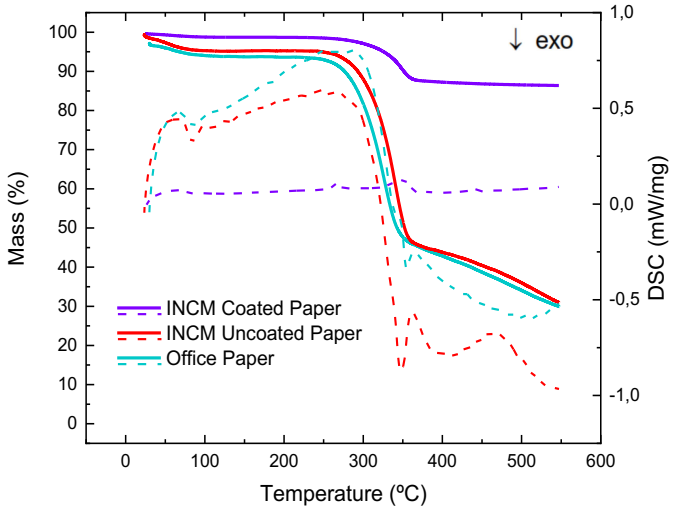

Figure 15 – TGA-DSC analysis of the paper substrates studied. For each paper in continuous line is represented the mass % and in dash the DSC.

With the purpose to summarize the substrates characterisation results, a qualitative comparison is made in

Table 7. INCM Coated paper seems to be the best substrate for paper electronics due to its low roughness and high temperature resistance. Although the Office paper and INCM Uncoated paper have more fibres and fillers, they can still be used as substrate, representing more ink scattering and absorption. In inkjet printing, for instance, those factors can be reduced by manipulating the printing parameters used.

Table 7 – Qualitative comparison between the three substrates in the techniques used to characterise them (❌ - Bad; ✔ - Average; ✔✔ - Good).

	SEM	Profilometry	Contact Angle	TGA
Office Paper	❌	❌	✔	✔
INCM Uncoated Paper	✔	✔	❌	✔
INCM Coated Paper	✔✔	✔✔	✔✔	✔✔

3.2 Inkjet ink characterisation

3.2.1 Absorbance

The absorbance spectrum for Sicrys I50T-13 is shown in Figure 16. The spectrum shows high absorbance values in the UV zone with the maximum peak of absorbance set at 320 nm. It means that for a wavelength of 320 nm the ink absorbs more energy. Consequently, the sintering is expected to be much faster for that wavelength.[35] Without the needed UV lamp, the sintering selected followed the supplier's method, 200 ºC for 30 minutes.

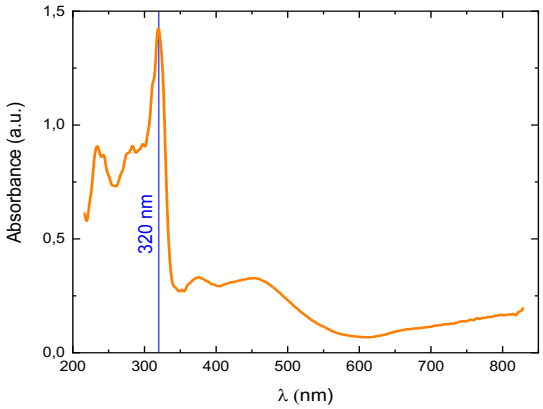

Figure 16 - Absorbance of Sicrys I50T-13 from 230 nm to 850 nm.

3.2.2 TGA-DSC Analysis

TGA-DSC measurements for the inkjet silver ink Sicrys I50T-13 are shown in Figure 17. At approximately 150 ºC the ink has lost half of its mass, starting at approximately 100 ºC. This not only confirms that the NPs loading is 50%, as said in the datasheet, but also gives the information that with 150 ºC the ink will be sintered. This test was only done with an ink sample, with the substrate this value needs to be higher since the temperature in the hot plate is applied in the substrate.

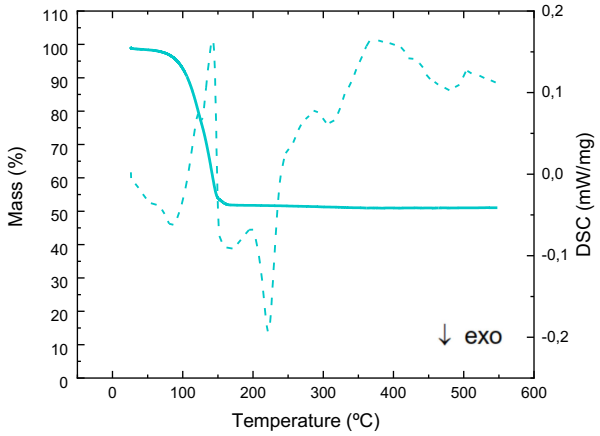

Figure 17 - TGA-DSC analysis of Sicrys I50T-13. In continuous line is represented the mass % and in dash the DSC.

3.2.3 Viscometer

The viscosity is a crucial parameter in printing techniques. For the Dimatix printhead used, the required ink viscosity values are comprehended between 10 and 20 cPs. Using values above the recommended can cause clogged nozzles and below the recommended can cause an uncontrolled continuous stream of ink.

The objective of this analysis is to study the evolution of the viscosity with increasing temperature. In Figure 18, can be observed that the viscosity tends to reduce with the temperature. With this, it can be established that the printer head needs a temperature of at least 27ºC and below 45ºC to be inside the recommended viscosity values range.

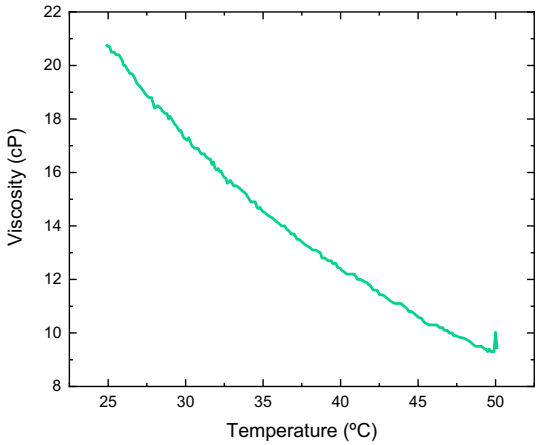

Figure 18 – Sicrys I50T-13 viscosity change, in the temperature range of 25 ºC to 50 ºC.

3.3 RFID Layout Optimisation for Inkjet Printing

In this chapter, only the bottom layer of the RFID antenna will be considered. The two top layers, as said before, only consist in an insulant bridge and a conductive path to pull the inner pad to outside.

The layout suffered several modifications over time to achieve the aimed resistance of 50 Ω as well as optimized printing conditions compatible with a mass production of RFID antennas using a sheet-to-sheet (S2S) or roll-to-roll (R2R) process. The most important objectives with the layout optimisation were to reduce of the printing time and the pad-to-pad resistance.

The layout evolution is shown in Figure 19 through Figure 21. Antenna A from Figure 19 represents the standard layout used in RFID applications and was adapted from [66]. This procedure was made for inkjet printing. This technique proves to be suitable to this purpose because there is no need to use a mask, the layout is uploaded to the printer software and after that, the printing can start. The design adjustments can be made by a design software by changing the characteristics of

the antenna, like the pad format, line thickness, spacing between the lines or the overall dimensions of the antenna like the length and width. The initial layout had a 52 × 52 mm size.

The antennas B, C and D represent alternative corner formats for the antennas because it was in the corners that the resistance increased more. So, with that in mind, the layout was changed adding more ink to the corners in those three different layouts.

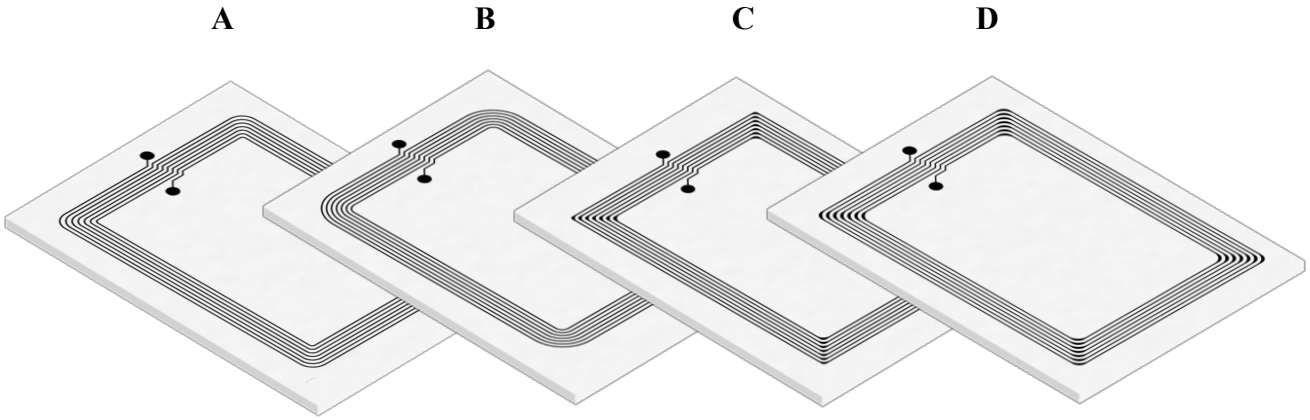

Figure 19 – RFID antennas layouts 52 × 52 mm. (A) Standard design (adapted from [66]), (B),(C) and (D) represent different corner designs.

Since the printing time was too long (approx. 30 minutes at 2000 dpi and 20 minutes at 1500 dpi), the width of the antenna design was reduced to half of the original size, that way the printing time of 1 layer decreased to half (15 minutes at 2000 dpi and 10 minutes at 1500 dpi approx.). With that, all the layouts A, B, C and D from Figure 19 were converted to half of the width, being then with 52 × 26 mm size, as shown in antennas E, F, G and H in Figure 20. When comparing these four layouts, the better layout proved to be the layout H, which have the same corner type as layout D from Figure 19.

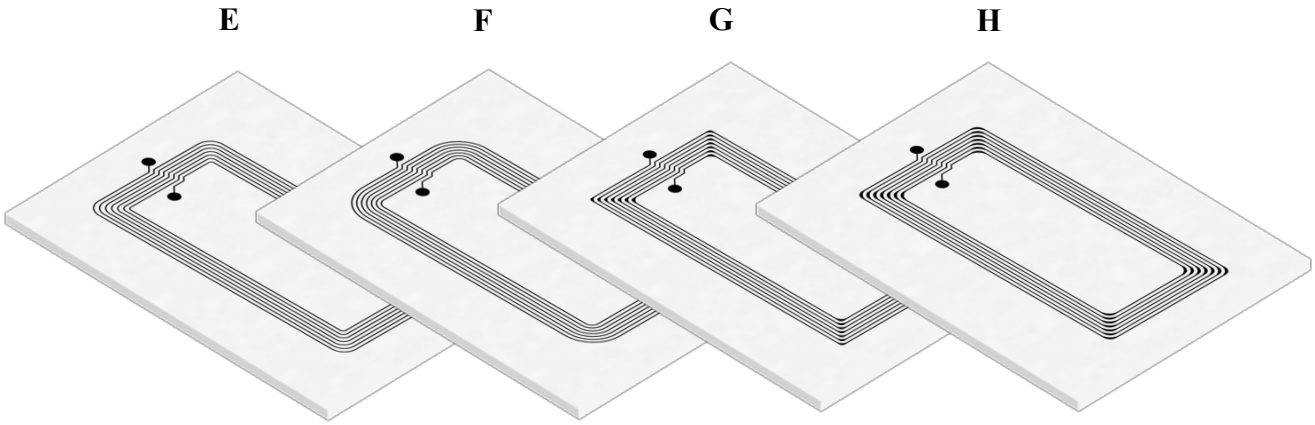

Figure 20 –RFID antennas layouts 52 × 26. (E) Standard design (adapted from [66]), (F),(G) and (H) represent different corner designs.

After optimising the corner type, the 45º angles between the pads were removed, since there was also an increase of resistance there, as shown in layout I from Figure 21. To reduce even more the resistance, the number of loops was reduced to 3. With that, not only the lines could be thicker (from 200 µm to 400 µm), but also the pad to pad track distance was also reduced. The format of the pads was also change due to the 45º angles presence and to increase the contact zone, as shown in layout J. Layout K has only one change, the increased distance between adjacent tracks to avoid short circuit due to ink scattering and absorption on the paper substrates. This is considered the final layout and was the chosen one to be reproduced by the three printing techniques.

The last layout presented, layout L, consists of a RFID antenna with the original size of layout A from Figure 19 (52 × 52 mm). This layout was designed to have a RFID antenna with the initial number of loops.

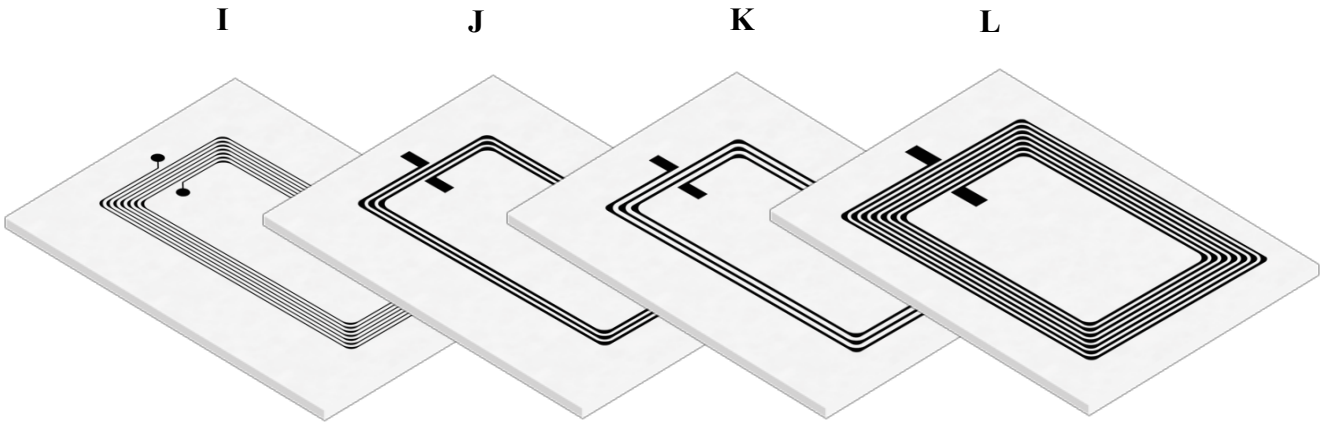

Figure 21 – RFID antenna layouts. (I) without 45º angle between pads, (J) with less loops and new pads, (K) with 600 µm spacing, (L) layout J the initial number of loops.

3.4 RFID Antennas Printing

3.4.1 Inkjet Printing

Concerning the printing direction, since the layout presents higher length in Y than X, printing direction Y was selected. Despite the resolution being the same in both directions, if the tracks are perpendicular to the direction they tend to have an increase in their thickness, due to the printer sweeps. That effect can be observed in Figure 22 where the two antennas represented differ only in the printing direction. The antenna in Figure 22 a) has been printed in Y direction and presents a vertical line thickness of 500 ± 28 µm. The horizontal lines have a thickness of 650 ± 85 µm. Concerning the Figure 22 b), vertical lines have 700 ± 21 µm and horizontal lines have 530 ± 34 µm. The layout design had a line thickness of 400 µm, these higher values have to do with the scattering of ink on the paper surface, paper absorption among other things.

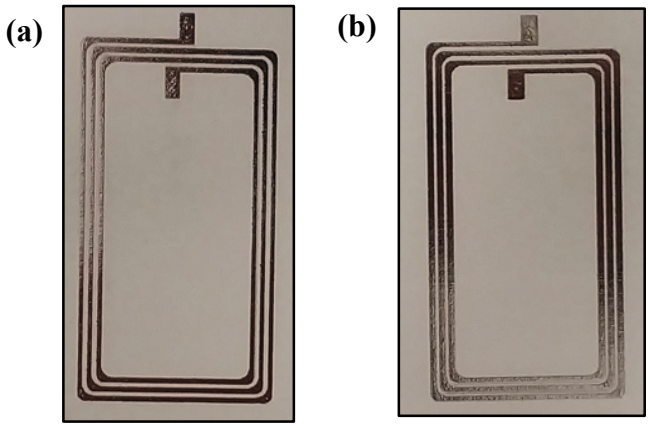

Figure 22 - RFID antennas with layout D2 printing in: a) Y direction and b) X direction.

The printing process was different for each substrate. Office paper and INCM Uncoated paper being more porous and having more fibres needed more layers of ink, the same did not happen with INCM Coated paper, because of its smoother surface, and as said before, more hydrophilic behaviour. For each substrate, in Table 8 are represented the printing parameters for the inkjet process on each substrate. In Figure 23 are represented the same antennas. These results are concerned only to the layout K from Figure 21.

Glass and PEN were used as reference for inkjet printing on non-porous substrates.

Table 8 – Inkjet printing parameters and resistance values for the best antennas for each substrate.

Substrate	**Substrate Temperature (°C)**	**Number of layers**	**Resolution (DPI)**	**Resistance (Ω)**
Office paper	75	3	1500	143
INCM Uncoated paper	60			134
INCM Coated paper	RT	2	2000	106
PEN	45	1	1500	88
Glass			2000	75

INCM Uncoated paper, represented in Figure 23 (b), presents a zone brown coloured at the right side. This behaviour occurs due to the hot plate sintering, it is paper ageing and represent paper degradation in that zone. The paper originally presents a yellow colour which is more noticeable post-sintering.

Concerning to the ink, it presents a low adhesion to glass substrate, with this having to do with superficial energy and, as the ink producer says in the datasheet, this ink is adequate to polymer substrates such as PEN, PET and PC. [58] In paper substrates ink adhesion is better than in glass due to the paper fibres absorption.

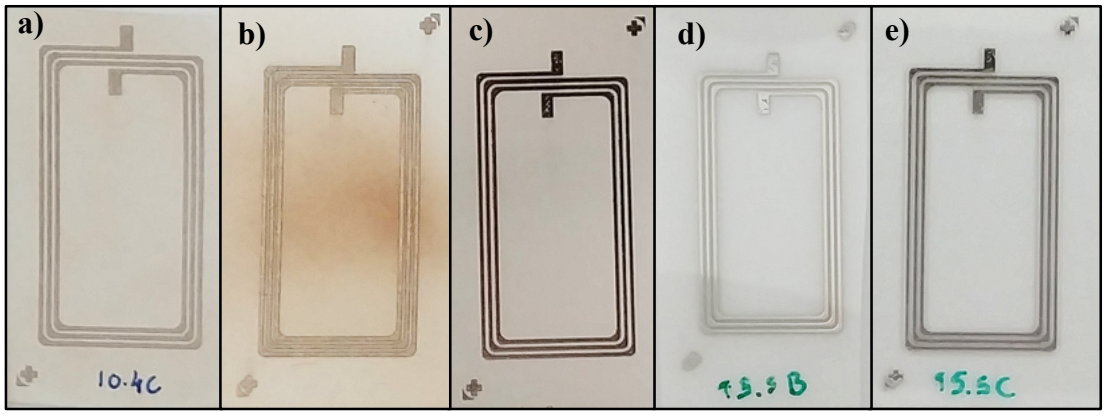

Figure 23 – Inkjet printed antennas for each substrate: a) Office paper; b) INCM Uncoated paper; c) INCM Coated paper; d) PEN; e) Glass.

3.4.2 **Screen Printing**

The layouts printed by screen printing were K and L from Figure 21 also shown in Figure 24 a) and b) respectively. Figure 24 c) to h) show the printed antennas from the Table 9 corresponding to the best results achieved in this technique for each paper substrate.

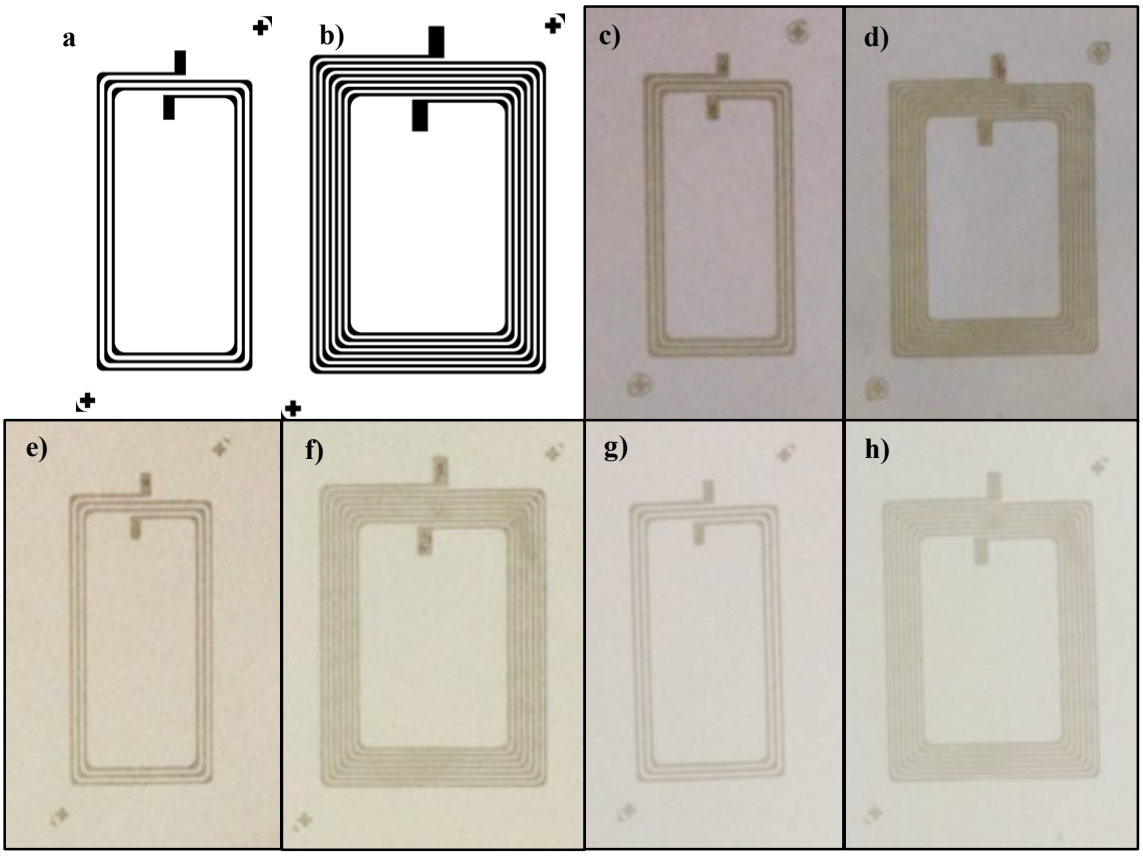

Figure 24 – RFID antenna layout K (a) and L (b); Screen printing RFID printed antennas for: (c) and (d) office paper; (e) and (f) INCM Uncoated paper; (g) and (h) INCM Coated paper.

The antennas produced by screen printing were expected to have less resistance than inkjet printed antennas due to the thickness of the printed tracks. In screen printing the ink is not

considered a solution but a paste due to its high viscosity, the deposition process only needs one layer and the results are highly related to the high NP content of the paste. In order to achieve even lower resistance values two printing layers were tested, but the results were significantly worst due to the ink scattering and adhesion to the mesh.

Table 9 - Screen printing best resistance values obtained for each paper substrate.

Paper	***Number of passages***	***Antenna K Resistance (Ω)***	***Antenna L resistance (Ω)***
Office paper	1	24	29
INCM Uncoated paper		29	34
INCM Coated paper		34	56

3.4.3 Flexographic Printing

Flexographic printing was carried out using layout K represented in Figure 21. The best results achieved were with anilox 4 cm^3/m^2. In Table 10 is represented the optimized parameters for the flexographic printing in all three substrates used. The number of passages consists is the number of layers deposited in the substrate and in order to obtain lower resistance this number can be increased. As one layer printing takes approximately 3 seconds, a high number of passages can be done without compromising the printing time of the overall process. The use of anilox 4 cm^3/m^2 and high number of passages with the ink solution of 2:1 is a compromise to transfer small quantities of ink to the substrate. The values presented in Table 10 can be altered, using more ink concentration and bigger aniloxes, such as 7 cm^3/m^2 or even 10 cm^3/m^2.

One situation to be avoided is the use of a bigger anilox with less ink concentration. A bigger anilox will mean more ink deposited and less ink concentration will mean a bigger solvent quantity. This will result in scattering and short circuit between tracks. Since the ink transferred is in bigger quantity when compared with inkjet, the substrate may also be damaged due to solvent absorption, even using more concentration than inkjet. The antennas presented in Table 10 are shown in

Figure 25.

Table 10 - Optimised parameters for each substrate by flexographic printing and achieved resistances.

Paper	**Number of passages**	**Velocity (m/min)**	**Pressure 1**	**Pressure 2**	**Resistance (Ω)**
Office paper	20	40	150	100	98
INCM Uncoated paper					109
INCM Coated paper	12				149

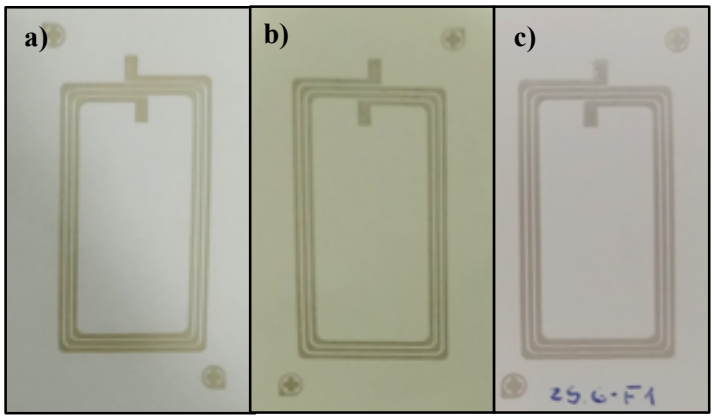

Figure 25- RFID antennas produced by flexographic printing in (a) office paper, (b) INCM Uncoated paper and (c) INCM Coated paper.

3.5 Comparison between the different printing techniques

To analyse the printing results and to know what the ink behaviour is in each substrate SEM images of the printing tracks were obtained. Figure 26 through Figure 28 present SEM images of the printing processes in each substrate. Images of the tracks in more detail can be observed in Annex C.

Inkjet printing results are shown in Figure 26. Although the fibres are covered with ink in Office paper and INCM Uncoated paper, there is no uniform layer as INCM Coated paper presents. This is related to the low quantity of ink deposited by this technique and the fibre absorption. In INCM Coated paper, this thin layer is formed, since there is a coating presence.

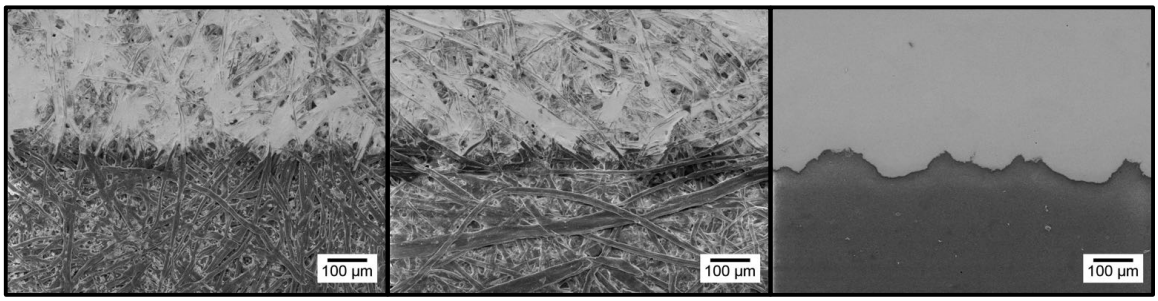

Figure 26 – SEM images of inkjet printing tracks for each paper substrate used. (a) Office paper; (b) INCM Uncoated paper; (c) INCM Coated paper.

For screen printing tracks, presented in Figure 27, the irregular shape is related to the mesh and the high ink viscosity. The fact that the fibres in Office paper and INCM Uncoated paper do not absorb the ink, as shown in inkjet printing, also increases this irregular shape tracks. All the papers studied show holes and cracks in the printed tracks, but in INCM Coated paper, this behaviour is more evident. Once again, this have to do with the coating presence and consequently less adhesion to the surface.

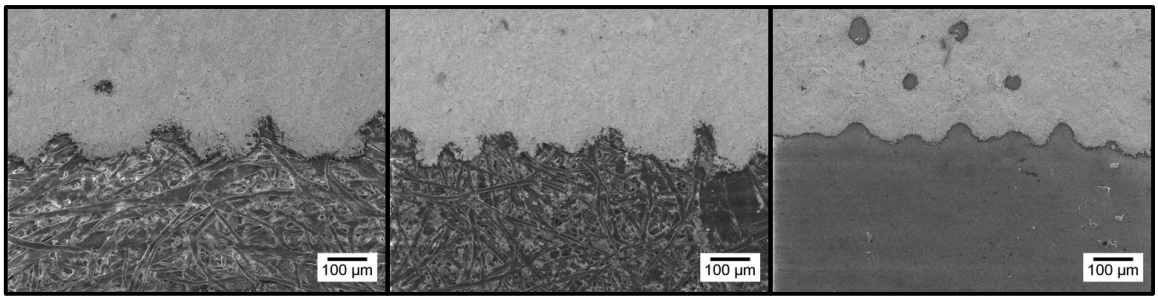

(a) **(b)** **(c)**

Figure 27 - SEM images of screen printing tracks for each paper substrate used. (a) Office paper; (b) INCM Uncoated paper; (c) INCM Coated paper.

Flexographic was the last technique analysed and it shows the best results in terms of track uniformity for all the papers studied, as shown in Figure 28. INCM Coated shows some scattering in the track edge. This confirms that there are some disadvantages in this substrate, once the adhesion of the inks to the substrate is low. This is caused by the contact between the substrate and the printer mask, to which the ink shows some adhesion and consequently not all the desired quantity is deposited in the substrate.

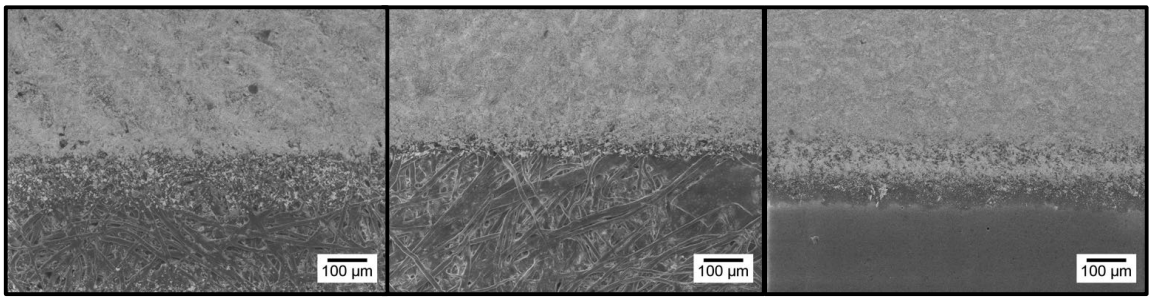

(a) **(b)** **(c)**

Figure 28 - SEM images of flexographic printing tracks for each paper substrate used. (a) Office paper; (b) INCM Uncoated paper; (c) INCM Coated paper.

As for a better comparison between the printing techniques, a qualitative assessment has been made for the used printing methods, considering some of the most important printing parameters. This is relevant when upscaling to mass manufacturing such as R2R processes. Inkjet printing resistance values can be decreased with a compromise between the number of layers and substrate temperature, although, the printing time will increase to obtain more track thickness.

The best results were achieved by screen printing, in which resistance values achieved less than 30 Ω. These results were expected due to the track thickness obtained.

Flexographic printing can still be optimized due to the high number of layer deposition. New Ag NP based ink may be tested due to the discontinuity of WB1078 production by Applied Ink Solutions.

A qualitative comparison between the printing techniques is presented in Table 11.

Table 11 - Qualitative comparison of printing parameters between printing techniques used. (× - Bad; ✓- Average; ✓✓- Good)

	Inkjet Printing	Flexographic Printing	Screen Printing
Resolution (DPI) Control	✓✓	×	×
Number of Layers	✓	×	✓✓
Pattern Transfer	✓✓	×	×
Printing velocity	×	✓✓	✓✓
Substrate Temperature	✓	×	×
Ink waste	✓✓	×	×
Scalability (R2R)	✓✓	✓✓	✓
Ink Sintering velocity	×	✓✓	✓✓

3.6 RFID Antenna Characterization

3.6.1 Printed RFID power harvesting

Using the Arduino and NFC reader RC522, the antennas were characterized measuring the voltage they produce. The results of that study are presented in Table 12.

The antenna that produced more voltage corresponded to the screen printed in INCM Coated paper with layout L, which presented 6.8 V. This value was expected to be higher than the others due to the number of loops. All the other antennas present voltage values around 4 V. Inkjet printed antenna in PEN presents a very low resistance value, although the produced voltage is not the expected. This may have to do with the substrate compatibility with RF waves, or even printing problems, whereby further PEN printings must be done to conclude something. The other two antennas that did not presented the expected values were both screen printed antennas, corresponding to the substrates INCM Coated and INCM Uncoated. This may have to do with the printing quality of the tracks or even problems concerning the RF measurements.

Table 12 - RFID printed antennas produced voltages.

	Paper	*Resistance (Ω)*	*Produced Voltage (V)*
Inkjet Printing	INCM Coated	143	4.2
	INCM Uncoated	134	4.0
	Office	106	4.6
	PEN	88	3.5
Flexographic printing	INCM Coated	149	4.3
	INCM Uncoated	109	4.0
	Office	98	4.2
Screen Printing	INCM Coated	34	2.8
	INCM Coated (layout L)	56	6.8
	INCM Uncoated	29	2.3
	Office	24	4.8

3.6.2 **Frequency Analysis**

In order to analyse the RFID antennas produced, frequency measurements were done, and the results are presented in Figure 29. The antennas described in this figure have the layout K (presented in Figure 21) and their impedance was studied from 1 to 60 MHz. The RFID antennas presented a relatively stable behaviour, where there is almost no variation in its impedance for lower values of frequency. For the desired frequency of 13.56 MHz, the antennas maintain low impedance values. This information can indicate that those antennas can do power harvesting from a source at that frequency and feed low voltage circuits.

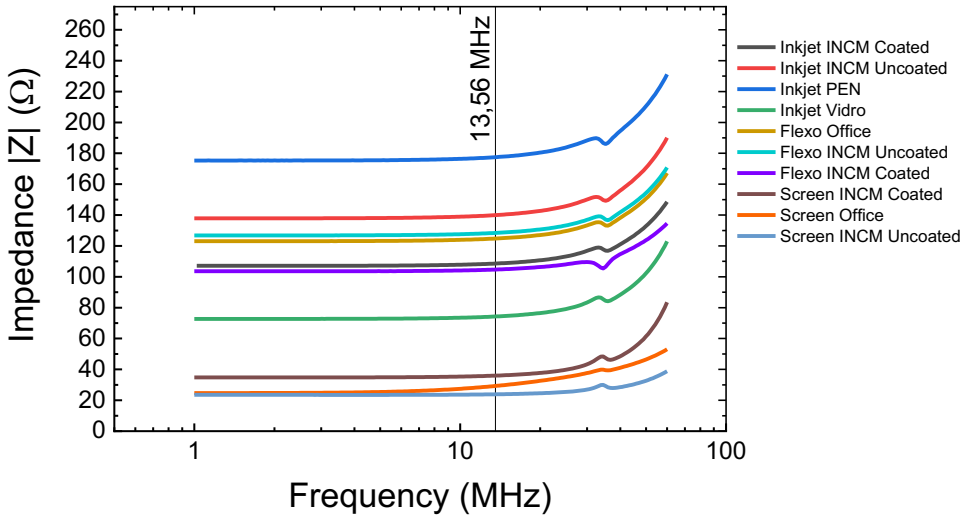

Figure 29 – Impedance analysis of the RFID antennas produced with layout K for each technique and each substrate.

A public transports card RFID antenna with a polymer based substrate, presented in Figure 8 (a), was studied to know the expected behaviour of a commercial antenna. The impedance in function of the frequency is represented in Figure 30, in black. In red is the printed antenna that showed the most similar behaviour to this commercial antenna. It was the screen-printed with 7 loops corresponding to layout L, that has as substrate INCM Coated Paper. This antenna is represented in Figure 24 and its printing conditions and resistance are shown in Table 9. The impedance in function of the frequency in linear scale can be seen in Annex D.

The screen printed antenna showed a highly similar impedance behaviour that demonstrates that RFID antennas can be printed in paper substrates with success. These results support that printed antennas are capable to replace the commercial ones with further investigation.

The impedance presented by the printed antenna is still a factor to reduce since that value is around 10 times higher than the commercial antenna.

The fact that layout L has more loops may indicate that the number of loops influences the RF behaviour of the antenna, in which more loops is more efficient. This was expected since the beginning of the optimisation process, even though the reason the number of loops was cut was due to the printing time in inkjet printing and ink scattering in that technique. Further tests are needed to verify these results and verify the expected behaviour of the printed RFID antennas.

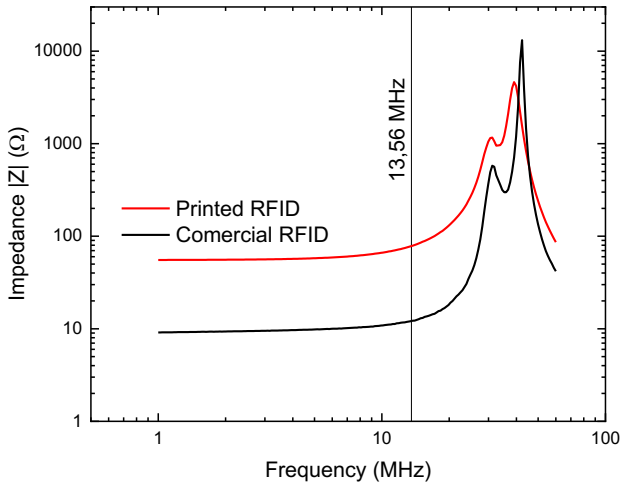

Figure 30 – Comparison between screen printed RFID with layout L and commercial RFID used in public transports card.

3.7 Final Device and Proof of Concept

3.7.1 3-layer RFID Antenna

To have antennas with all the layers printed, the screen printing technique was selected due to having the best results in terms of resistance and a faster sintering process. The procedure consisted in a 3-layer process. Firstly, the deposition of the antenna (coil), followed by the insulating path to

pull the inner contact to outside of the coil, which is the last layer. In Figure 31 below is represented the completed antenna printed by screen printing.

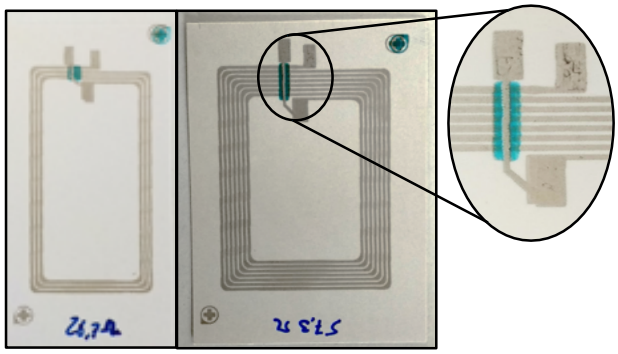

Figure 31 - 3-layer screen printed RFID antenna on INCM Coated paper. In a) is represented Layout K and in b) Layout L (with more loops); c) shows an amplified image of the insulant bridge printed.

As said by the ink supplier, the insulant ink and the Ag NP ink have good adhesion between them, which presented a major advantage in this process. The sintering processes of all layers followed the respective inks datasheet.

3.7.2 **RFID Antenna Testing**

Nowadays, majority of smartphones have an NFC (Near Field Communication) source.[67] This utility can be used for many applications, like fast payments, transports, information sharing, communication, among others. This NFC source was used as a RF wave emitter in this proof of concept. That could only happen because the produced RFID were optimized for 13.56 MHz and NFC shares the same frequency.

The RFID antennas received the signal and produced a certain voltage with that signal. The functional principle is the same of a Tesla Coil. If an electric current or wave goes through an inductor, energy is stored at the coil and can be used. At a certain proximity to the source, where the voltage is higher, the LED is blinking and with distance increase the LED does not blink anymore and stays OFF, presented in Figure 32.

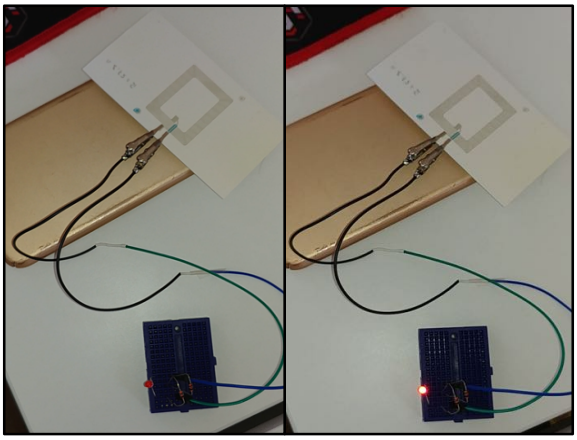

Figure 32 - Blinking LED obtained by RFID antenna power harvesting a smartphone NFC source. The LED blinked, in the left LED is OFF and in the right LED is ON.

4 Conclusions and Future Perspectives

4.1 Conclusions

Paper, as a substrate for electronics, is proving to be equal or more efficient than traditional materials and an example of that are the RFID antennas produced in this work. This low-cost substrate associated with the powerful advances of printing techniques and conductive inks is still an area in discovery. It can present lot of solutions, not only for the IoT subject, but also for other areas, such as biosensors, microfluidics, solar cells, transistors, among other on-paper technologies.

Three paper substrates were used in this thesis: Office paper, INCM Uncoated paper and INCM Coated paper. In terms of substrate characterization, INCM Coated paper presented a smoother surface due to the coating presence. This fact is a major advantage when it comes to the ink absorption, but a big disadvantage when regarding ink adhesion. For the last two, the office paper presented more fibres than INCM Uncoated paper, although, the last one presented more fillers.

Three different printing techniques were used to produce the antennas. Firstly, the layout was optimised for inkjet printing and then a comparison with flexography and screen printing was made. Inkjet proved a very good method for layout optimisation because it is a mask-free technique. Fast design corrections and alterations can be performed, without the need of producing or buying a new mask for every layout. Although, this technique is slower when compared to the other two techniques. Besides being faster, screen printing proved to be the best technique to produce RFID antennas, as it was expected due to the nature of the process (ink viscosity, NP loading, printing velocity), being the only technique to reach resistance values below 50 Ω. Also, its fast sintering presented a major advantage when compared with the other two procedures. Concerning the flexographic printing, although, low resistance values were obtained, optimisations still need to be done due to the high number of layers necessary to have low resistance working antennas. A compromise between ink viscosity, number of layers and anilox volume must be done to achieve better resistance values with less layers.

Concerning the layout, after optimisation the layout L presented the best behaviour when compared with a commercial RFID antenna. This could be due to the increased numbers of loops. This antenna layout was also the one that produced more voltage reaching 6,8V. This voltage was used in a proof of concept where a LED was turned on, just with an NFC power source and the antenna.

Functional RFID antennas were produced with all the techniques presented: inkjet, flexography and screen printing in all the paper substrates used. All these three processes present a R2R or S2S mass manufacturing in industrial systems which is a major advance in the production of devices at low-cost using green technologies.

4.2 Future Perspectives

Although this study objective was to optimize the printing of RFID antennas, there is a need to study the relation between the layouts and the generated voltages in more detail. A possible approach is to run simulations with a software and discover the layout that harvests more energy. After that, modifications in the design can be made according to the technique used. Other possibility, is the use of hybrid circuits, joining printing electronics with an integrated circuit (IC). This process can make the antenna semi-passive or active, an all-new area of study with more applications and higher operation range.

Since Layout L presented the best results in terms of produced voltage and impedance measurements, further tests in this layout are needed to achieve more conclusions. For instance, gain measurements, distance of operation, phase, reactance, among other characterisation processes can be done.

Concerning the techniques used, flexographic printing can still be optimised with a reduction of printing layers using different ink viscosities and anilox volumes. In screen printing, the automatic version of this process is a must to achieve higher velocity. Furthermore, this technique brings more automaticity and camera-assisted alignment, which are great advantages, especially when the objective is the 3-layer printing. Regarding inkjet printing, since the sintering is a drawback, the speed can be increased through UV sintering at 320 nm using a UV lamp. To accelerate the inkjet printing process multiple printheads or more nozzles can be used, since increasing the printing speed brings spraying and less accurate results.

Concerning the 3-layer layout, inkjet printing and flexographic printing tests can be done using insulant inks as the one used in screen-printing. Different inks can be tested to reduce the sintering times and to achieve lowest resistance values. Another approach is Pen-on-Paper (PoP) that consists in a regular pen in which the cartridge is changed by adding a formulated or a commercial ink. [68] The ink sintering is as fast as in screen printing and can also be automatized by making a setup similar to a conventional 3D printer system. This method can be used to substitute the top layer of the process.

The effect of absorption and ink scattering can be reduced, obtaining the antenna with the wanted dimensions. Therefore, a study of line thickness and printing conditions is essential for a reduction of the equivalent percentage of ink that scatters, for each substrate. Afterwards, the modifications can be made in a design software. Some of the printing conditions to be considered are: printing direction, resolution, velocity, among others.

5 Bibliography

[1] R. P. Feynman, “There ’ s Plenty of Room at the Bottom,” vol. I, no. I, pp. 60–66, 1992.

[2] K. Dabhi and A. Maheta, “Internet of Nano Things-The Next Big Thing,” vol. 7, no. 4, pp. 10602–10604, 2017.

[3] J. Gubbi, R. Buyya, S. Marusic, and M. Palaniswami, “Internet of Things (IoT): A vision, architectural elements, and future directions,” *Futur. Gener. Comput. Syst.*, vol. 29, no. 7, pp. 1645–1660, 2013.

[4] T. Kaukalias and C. Periklis, *Internet of Things (IoT), Encyclopedia of Information Science and Technology*, Third Edit. 2015.

[5] X. Jia, Q. Feng, T. Fan, and Q. Lei, “RFID Technology and Its Applications in Internet of Things (IOT),” pp. 1282–1285, 2012.

[6] M. Borgese, F. A. Dicandia, F. Costa, S. Genovesi, and G. Manara, “An Inkjet Printed Chipless RFID Sensor for Wireless Humidity Monitoring,” *IEEE Sens. J.*, vol. 17, no. 15, pp. 4699–4707, 2017.

[7] B. Nath, F. Reynolds, and R. Want, “RFID Technology and Applications,” *Pervasive Comput. IEEE*, vol. 5, no. 1, pp. 22–24, 2006.

[8] Y. Jin *et al.*, “A Power Management Scheme for Wirelessly- Powered RFID tags with Inkjet-Printed Display,” pp. 180–185.

[9] D. Fengel and G. Wegener, *Wood: chemistry, ultrastructure, reactions*. De Gruyter, 2011.

[10] K. Sindhu, R. Prasanth, and V. K. Thakur, *Medical Applications of Cellulose and its Derivatives: Present and Future*. 2014.

[11] H. J. Skinner, “Cellulose in Industry,” *Ind. Eng. Chem.*, vol. 24, no. 6, pp. 694–704, Jun. 1932.

[12] M. Laka and S. Chernyavskaya, “Obtaining microcrystalline cellulose from softwood and hardwood pulp,” *BioResources*, vol. 2, no. 4, pp. 583–589, 2007.

[13] P. Bajpai, “Basic Overview of Pulp and Paper Manufacturing Process BT - Green Chemistry and Sustainability in Pulp and Paper Industry,” P. Bajpai, Ed. Cham: Springer International Publishing, 2015, pp. 11–39.

[14] F. Kačík, D. Kačíková, M. Jablonský, and S. Katuščák, “Cellulose degradation in newsprint paper ageing,” *Polym. Degrad. Stab.*, vol. 94, no. 9, pp. 1509–1514, 2009.

[15] D. Tobjörk and R. Österbacka, “Paper electronics,” *Adv. Mater.*, vol. 23, no. 17, pp. 1935–

1961, 2011.

[16] H. Sandberg, C. Gaspar, and L. Hakola, *Integrated Printed Hybrid Electronics on Paper*. 2014.

[17] R.H.Leach, *The Printing Ink Manual*. 1993.

[18] S. Khan, L. Lorenzelli, R. Dahiya, and S. Member, "Technologies for Printing Sensors and Electronics over Large Flexible Substrates : A Review," no. December, 2014.

[19] M. Jung *et al.*, "All-Printed and roll-to-roll-printable 13.56-MHz-operated 1-bit RF tag on plastic foils," *IEEE Trans. Electron Devices*, vol. 57, no. 3, pp. 571–580, 2010.

[20] K. Suganuma, *Introduction to Printed Electronics*, vol. 74. 2014.

[21] B. Derby, "Inkjet Printing of Functional and Structural Materials : Fluid Property Requirements , Feature Stability , and Resolution."

[22] H. Sirringhaus and T. Shimoda, "Inkjet Printing of Functional Materials," *MRS Bull.*, vol. 28, no. 11, pp. 802–806, 2003.

[23] W. Thomson and Lord Kelvin, "Inkjet printing 1.," no. 1, pp. 1–21.

[24] B. W. Jo, A. Lee, K. H. Ahn, and S. J. Lee, "Evaluation of jet performance in drop-on-demand (DOD) inkjet printing," *Korean J. Chem. Eng.*, vol. 26, no. 2, pp. 339–348, 2009.

[25] M. Singh, H. M. Haverinen, P. Dhagat, and G. E. Jabbour, "Inkjet printing-process and its applications," *Adv. Mater.*, vol. 22, no. 6, pp. 673–685, 2010.

[26] B. Derby, "Inkjet Printing of Functional and Structural Materials: Fluid Property Requirements, Feature Stability, and Resolution," *Annu. Rev. Mater. Res.*, vol. 40, no. 1, pp. 395–414, Jun. 2010.

[27] B. J. De Gans, P. C. Duineveld, and U. S. Schubert, "Inkjet printing of polymers: State of the art and future developments," *Adv. Mater.*, vol. 16, no. 3, pp. 203–213, 2004.

[28] J. Izdebska, *Flexographic Printing*. Elsevier Inc., 2015.

[29] J. Olkkonen, K. Lehtinen, and T. Erho, "Flexographically printed fluidic structures in paper," *Anal. Chem.*, vol. 82, no. 24, pp. 10246–10250, 2010.

[30] P. F. Moonen, I. Yakimets, and J. Huskens, "Fabrication of Transistors on Flexible Substrates : from Mass-Printing to High-Resolution Alternative Lithography Strategies," pp. 1–16, 2012.

[31] F. C. Krebs *et al.*, "A complete process for production of flexible large area polymer solar cells entirely using screen printing-First public demonstration," *Sol. Energy Mater. Sol. Cells*, vol. 93, no. 4, pp. 422–441, 2009.

[32] P. E. S. Burr, “United States Patent (19) U . S . Patent Dec . 20 , 1977,” no. 19, 1977.

[33] M. L. Allen, K. Jaakkola, K. Nummila, and H. Seppa, “Applicability of metallic nanoparticle inks in RFID applications,” *IEEE Trans. Components Packag. Technol.*, vol. 32, no. 2, pp. 325–332, 2009.

[34] K. Rajan, I. Roppolo, A. Chiappone, S. Bocchini, D. Perrone, and A. Chiolerio, “Silver nanoparticle ink technology: state of the art,” *Nanotechnol. Sci. Appl.*, vol. 9, pp. 1–13, Jan. 2016.

[35] D. Tobjörk *et al.*, “IR-sintering of ink-jet printed metal-nanoparticles on paper,” *Thin Solid Films*, vol. 520, no. 7, pp. 2949–2955, 2012.

[36] M. Rizwan *et al.*, “Possibilities of Fabricating Copper-Based RFID Tags with Photonic-Sintered Inkjet Printing and Thermal Transfer Printing,” *IEEE Antennas Wirel. Propag. Lett.*, vol. 16, pp. 1828–1831, 2017.

[37] I. Ortego, N. Sanchez, J. Garcia, F. Casado, D. Valderas, and J. I. Sancho, “Inkjet printed planar coil antenna analysis for NFC technology applications,” *Int. J. Antennas Propag.*, vol. 2012, 2012.

[38] U. Caglar, K. Kaija, and P. Mansikkamäki, “Analysis of mechanical performance of silver inkjet-printed structures,” *2008 2nd IEEE Int. Nanoelectron. Conf. INEC 2008*, pp. 851–856, 2008.

[39] S. Amendola, A. Palombi, and G. Marrocco, “Inkjet Printing of Epidermal RFID Antennas by Self-Sintering Conductive Ink,” *IEEE Trans. Microw. Theory Tech.*, vol. 66, no. 3, pp. 1561–1569, 2018.

[40] R. D. Mancosu, J. A. Q. Quintero, and R. E. S. Azevedo, “Sintering, in different temperatures, of traces of silver printed in flexible surfaces,” in *2010 11th International Thermal, Mechanical & Multi-Physics Simulation, and Experiments in Microelectronics and Microsystems (EuroSimE)*, 2010, pp. 1–5.

[41] A. Iswarya. and B. Priyalakshmi, “Design and fabrication of rfid antenna tag using paper substrate for low-cost RFID applications,” in *2016 Online International Conference on Green Engineering and Technologies (IC-GET)*, 2016, pp. 1–6.

[42] R. Singh, E. Singh, and H. S. Nalwa, “Inkjet printed nanomaterial based flexible radio frequency identification (RFID) tag sensors for the internet of nano things,” *RSC Adv.*, vol. 7, no. 77, pp. 48597–48630, 2017.

[43] J. T. Carvalho, “Field-Effect Transistors Based on Zinc Oxide Nanoparticles,” FCT-UNL, 2015.

[44] V. Subramanian, P. C. Chang, J. B. Lee, S. E. Molesa, and S. K. Volkman, "Printed organic transistors for ultra-low-cost RFID applications," *IEEE Trans. Components Packag. Technol.*, vol. 28, no. 4, pp. 742–747, 2005.

[45] A. Vena, L. Sydänheimo, L. Ukkonen, and M. M. Tentzeris, "A fully inkjet-printed chipless RFID gas and temperature sensor on paper," *2014 IEEE RFID Technol. Appl. Conf. RFID-TA 2014*, vol. 2, pp. 115–120, 2014.

[46] H. Lehpamer, "5. Components of the RFID System," *RFID Des. Princ.*, pp. 133–201, 2008.

[47] H. He, J. Tajima, L. Sydanheimo, H. Nishikawa, L. Ukkonen, and J. Virkki, "Inkjet-printed antenna-electronics interconnections in passive UHF RFID tags," *IEEE MTT-S Int. Microw. Symp. Dig.*, pp. 598–601, 2017.

[48] K. Finkenzeller and R. Waddington, *RFID Handbook*. 2003.

[49] C. Ramade, S. Silvestre, F. P. Delannoy, and B. Sorli, "Thin film HF RFID tag deposited on paper by thermal evaporation," *Int. J. Radio Freq. Identif. Technol. Appl.*, vol. 4, no. 1, p. 49, 2012.

[50] M. Koller *et al.*, "Printed Flexible RFID Label with CMOS Temperature and Humidity Sensors Contact person :," p. 8401, 2002.

[51] S. Merilampi, L. Ukkonen, L. Sydänheimo, P. Ruuskanen, and M. Kivikoski, "Analysis of Silver Ink Bow-Tie RFID Tag Antennas Printed on Paper Substrates," *Int. J. Antennas Propag.*, vol. 2007, pp. 1–9, 2007.

[52] T. Çiftçi, B. Karaosmanoğlu, and Ergül, "Low-cost inkjet antennas for RFID applications," *IOP Conf. Ser. Mater. Sci. Eng.*, vol. 120, no. 1, 2016.

[53] D. Deganello, J. A. Cherry, D. T. Gethin, and T. C. Claypole, "Patterning of micro-scale conductive networks using reel-to-reel flexographic printing," *Thin Solid Films*, vol. 518, no. 21, pp. 6113–6116, 2010.

[54] "Via Verde." [Online]. Available: https://www.viaverde.pt/.

[55] "Indentificador Via Verde." [Online]. Available: https://fleetmagazine.pt/2011/05/09/calvador-caetano-vende-identificadores-da-via-verde-em-concessionarios/.

[56] "INAPA Superspeed A4/80." [Online]. Available: https://inapaportugal.pt/202304-inapa-tecno-super-speed-a4-80#.W6hBBWhKh1c.

[57] "INCM - Imprensa Nacional-Casa da Moeda." [Online]. Available: https://www.incm.pt/portal/index.jsp.

[58] PVnanocell, “Product Data Sheet,” pp. 1–2, 1999.

[59] “RK Printcoat Flexiproof 100/UV.” [Online]. Available: https://www.rkprint.com/products/flexiproof-100-uv/.

[60] Applied Ink Solutions, “TECHNICAL DATA SHEET WB - 1078 Water - Based Silver Conductive Ink,” pp. 10–11.

[61] SunChemicals, “CRSN2442 Conductive Silver Ink Datasheet,” no. October 2013, pp. 1–5.

[62] SunChemicals, “CFSN6057 UV Flexible Coverlay Datasheet,” no. October 2013, pp. 4–7.

[63] “Industrial Efficiency Technology Database.” [Online]. Available: http://ietd.iipnetwork.org/content/mechanical-pulping.

[64] R. Barras, “Cellulose-based composites as functional conductive materials for printed electronics,” 2015.

[65] A. Pimentel, A. Samouco, D. Nunes, A. Araújo, R. Martins, and E. Fortunato, “Ultra-fast microwave synthesis of ZnO nanorods on cellulose substrates for UV sensor applications,” *Materials (Basel).*, vol. 10, no. 11, pp. 4–10, 2017.

[66] NXP, “NTAG Antenna Design Guide,” no. April, pp. 1–47, 2016.

[67] “NFC World.” [Online]. Available: https://www.nfcworld.com/nfc-phones-list/.

[68] J. R. C. de O. S. Ribas, “Optimisation of Zinc Oxide Inks for Pen on Paper Transistors,” FCT-UNL, 2017.

6 Annex

Annex A- EDS Mapping of Paper Substrates

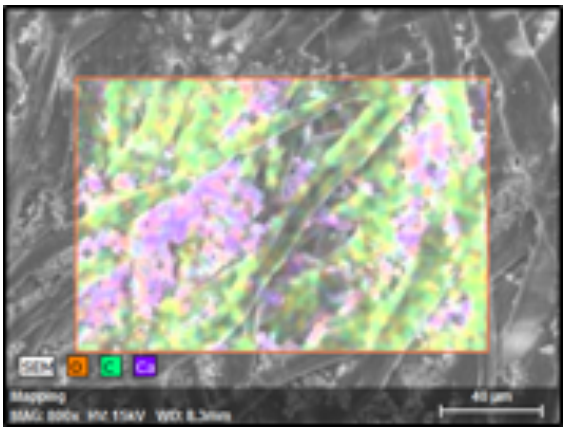

Figure 33 - EDS mapping of Office paper.

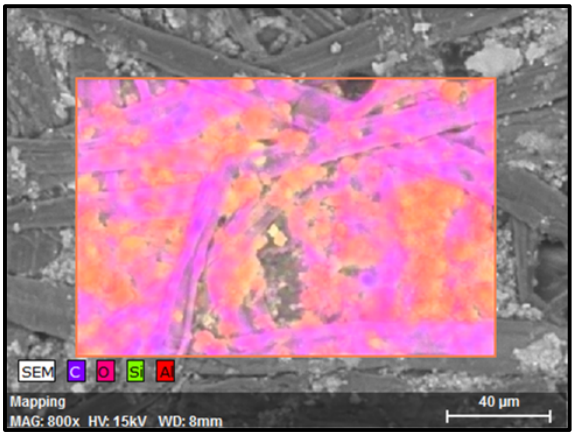

Figure 34 - EDS mapping of INCM Uncoated paper.

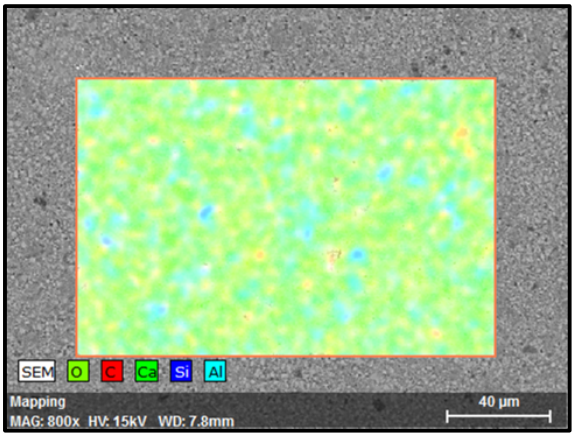

Figure 35 - EDS mapping of INCM Coated paper.

Annex B-INCM Coated Paper Cross-section

Figure 36 - SEM-EDS imaging and spectrum of INCM Coated paper cross-sectionFigure 36 below represented, there is a layer with different morphology at the top of the analysis zone (orange rectangle). The EDS scanning show a high Ca percentage, as well as highly defined peaks in the spectrum of the analysis zone confirms the existence of a coating in this paper substrate. This Ca presence indicates that the coating is $CaCO_3$, a commonly used paper coater.

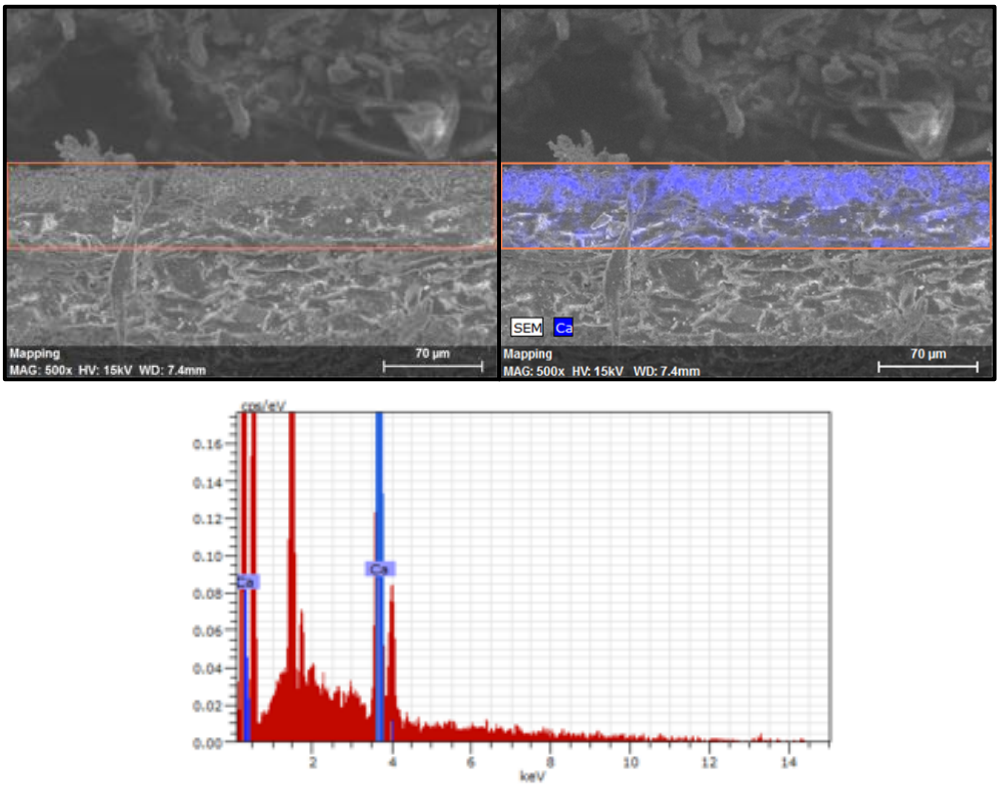

Figure 36 - SEM-EDS imaging and spectrum of INCM Coated paper cross-section

Annex C- SEM images of the printed tracks

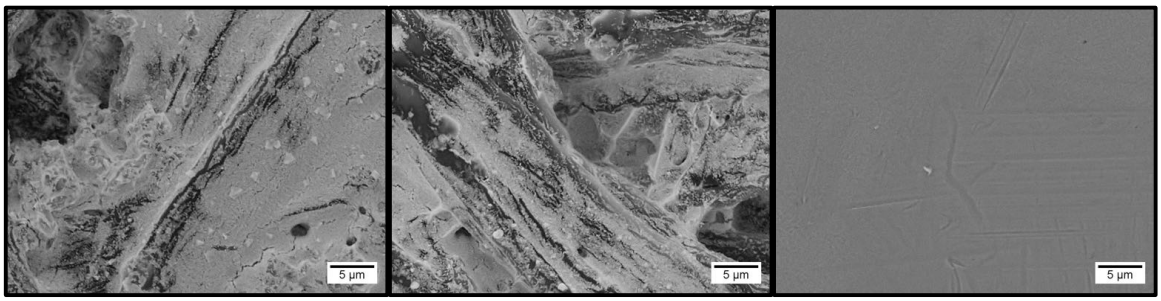

(a) **(b)** **(c)**

Figure 37 - SEM images of inkjet printed ink tracks on (a) Office paper; (b) INCM Uncoated paper; (c) INCM Coated paper.

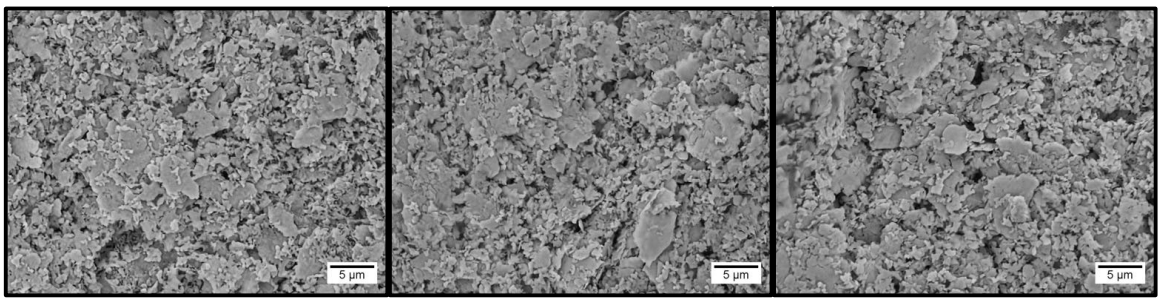

(a) **(b)** **(c)**

Figure 38 - SEM images of screen printed tracks on (a) Office paper; (b) INCM Uncoated paper; (c) INCM Coated paper.

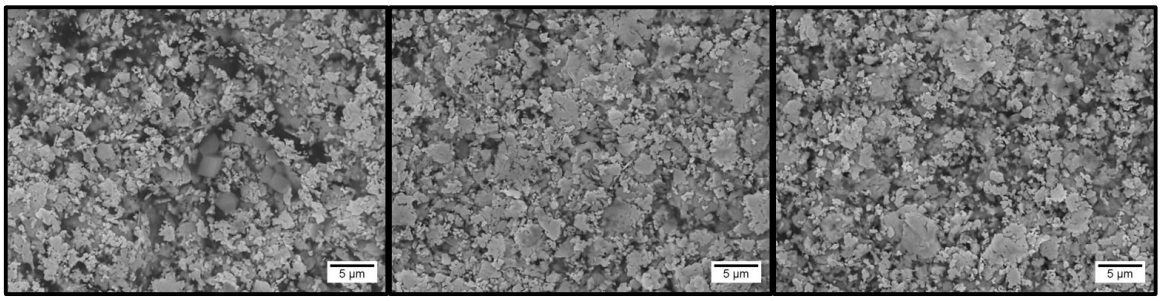

(a) **(b)** **(c)**

Figure 39 - SEM images of flexographic printed tracks on (a) Office paper; (b) INCM Uncoated paper; (c) INCM Coated paper.

Annex D- Impedance vs Frequency in linear scale

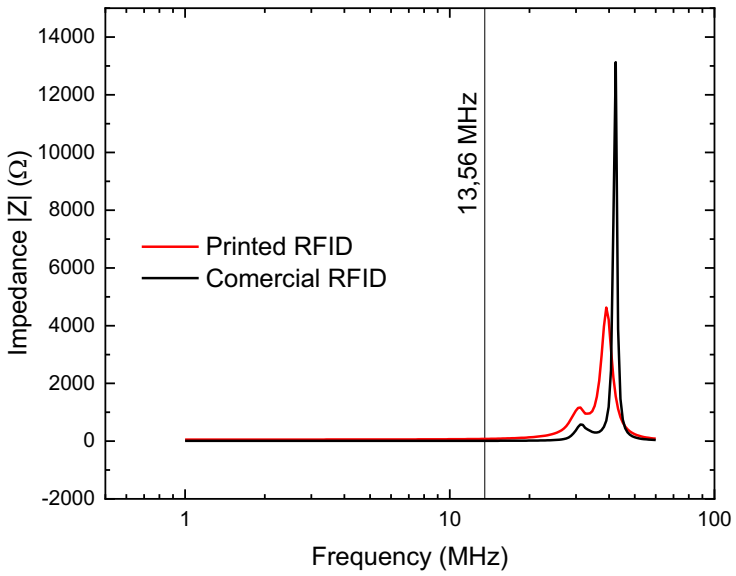

Figure 40 - Comparison between screen printed RFID with layout L and commercial RFID used in public transports card with the impedance in linear scale.